

# Operational resource theory of imaginarity

Kang-Da Wu,<sup>1,2</sup> Tulja Varun Kondra,<sup>3</sup> Swapan Rana,<sup>3,4</sup> Carlo Maria Scandolo,<sup>5,6</sup>  
Guo-Yong Xiang,<sup>1,2,\*</sup> Chuan-Feng Li,<sup>1,2</sup> Guang-Can Guo,<sup>1,2</sup> and Alexander Streltsov<sup>3,†</sup>

<sup>1</sup>*CAS Key Laboratory of Quantum Information, University of Science and Technology of China, Hefei 230026, People's Republic of China*

<sup>2</sup>*CAS Center For Excellence in Quantum Information and Quantum Physics, University of Science and Technology of China, Hefei, 230026, People's Republic of China*

<sup>3</sup>*Centre for Quantum Optical Technologies, Centre of New Technologies, University of Warsaw, Banacha 2c, 02-097 Warsaw, Poland*

<sup>4</sup>*S. N. Bose National Centre for Basic Sciences, JD Block, Sector III, Kolkata 700106, India*

<sup>5</sup>*Department of Mathematics & Statistics, University of Calgary, Calgary, AB, T2N 1N4, Canada*

<sup>6</sup>*Institute for Quantum Science and Technology, University of Calgary, Calgary, AB, T2N 1N4, Canada*

Wave-particle duality is one of the basic features of quantum mechanics, giving rise to the use of complex numbers in describing states of quantum systems, their dynamics, and interaction. Since the inception of quantum theory, it has been debated whether complex numbers are actually essential, or whether an alternative consistent formulation is possible using real numbers only. Here, we attack this long-standing problem both theoretically and experimentally, using the powerful tools of quantum resource theories. We show that – under reasonable assumptions – quantum states are easier to create and manipulate if they only have real elements. This gives an operational meaning to the resource theory of imaginarity, for which we identify and answer several important questions. This includes the state-conversion problem for all qubit states and all pure states of any dimension, and the approximate imaginarity distillation for all quantum states. As an application, we show that imaginarity plays a crucial role for state discrimination: there exist quantum states which can be perfectly distinguished via local operations and classical communication, but which cannot be distinguished with any nonzero probability if one of the parties has no access to imaginarity. This phenomenon proves that complex numbers are an indispensable part of quantum mechanics, and we also demonstrate it experimentally with linear optics.

Complex numbers, originated in mathematics, are widely used in mechanics, electrodynamics, and optics, allowing for an elegant formulation of the corresponding theory. The rise of quantum mechanics as a unified picture of waves and particles further strengthened the prominent role of complex number in physics. Indeed, the imaginary unit  $i$  appears in many formulas in quantum theory, notably in Schrödinger equation describing the time evolution of a quantum system, and is of fundamental importance in quantum physics and quantum information science.

According to the postulates of quantum mechanics, a state of a quantum system is described by a wave function  $\Psi(x) = |\Psi(x)| e^{-i\phi(x)}$  with probability amplitude  $|\Psi(x)|^2$  and phase  $\phi(x)$ . The wave-based point of view provides an important set of tools for the formulation and construction of quantum physics. Therefore it is natural to ask whether the complex arithmetic in quantum mechanics, arising from the imaginary part of  $e^{i\phi}$  is necessary to describe the fundamental properties and dynamics of a quantum system. In other words, can quantum physics be restated in a formalism using real numbers only? One approach to address this question is to use the standard rules of quantum mechanics, but to enforce all states and measurement operators to have real elements only [1–9]. The aim of this approach is then to find physical effects and applications, which are possible in standard quantum mechanics, but impossible in its version restricted to real num-

bers [10, 11]. It has been noted that this real-vector-space quantum theory is fundamentally different from the standard one from various aspects, e.g., it is bilocally tomographic [3], a rebit (real qubit) can be maximally entangled with many rebits [4, 6, 7], and it allows optimal transport of information from preparation to measurement [8].

Another reason to distinguish between complex and real quantum states is the effort to establish them in experimental setups. An important example is polarization-encoded photonic system, where we can realize an arbitrary rotation around the  $y$ -axis by a single half-wave plate, while for a rotation around the  $z$ -axis two additional quarter-wave plates are needed. The fact that a certain type of transformations is easy to perform is the basic feature of any quantum resource theory [12–14]. This justifies the study of the *resource theory of imaginarity* [15], using the framework of general quantum resource theories, which has been successfully applied to investigate basic properties and applications of quantum entanglement [16], quantum coherence [17], and quantum thermodynamics [18, 19]. This framework is based on the idea that there is a restriction on the operations on a quantum system, dictated by the physical setting. One then studies which conversions between states are possible under this restriction.

The aim of this work is twofold. Firstly, we provide the resource theory of imaginarity with an operational meaning, discussing the experimental role of complex and real operations, i.e., quantum operations which do not create imaginarity. Secondly, we identify and answer several important questions within this theory, and provide a concrete experimental application with linear optics. This includes the state-conversion

\* [gyxiang@ustc.edu.cn](mailto:gyxiang@ustc.edu.cn)

† [a.streltsov@cent.uw.edu.pl](mailto:a.streltsov@cent.uw.edu.pl)

problem, namely characterizing the interconversion between quantum states via real operations. We provide a complete solution to the single-shot state conversion problem between single-qubit mixed states. For arbitrary pure states, we evaluate the optimal probability of their interconversion. We also introduce the task of approximate imaginarity distillation, and present an optimal distillation procedure for all mixed states.

As an application, we show that imaginarity plays a crucial role for local quantum state discrimination, when complex numbers are allowed in the measurement. We show that there exist real bipartite states which can be perfectly distinguished via local operations and classical communication (LOCC), but which cannot be distinguished with any non-zero probability via LOCC restricted to real local measurements. In the context of quantum tomography, a similar effect has been observed previously in [10]. We provide a theoretical framework for studying local state discrimination, and find the advantage of local complex measurements which outperform real local measurements. By experimentally measuring the optimal distinguishing probability for different families of mixed states, our results clearly demonstrate that complex numbers play a distinguished role in quantum theory, allowing for phenomena which would not be possible with real quantum mechanics alone.

## RESULTS

*Resource theory of imaginarity*—The first step to formulating any resource theory is to identify the free states of the theory, i.e. quantum states which, within the theory under study, can be created at no cost. Similar to the resource theory of coherence [17, 20], we specify a particular basis  $\{|j\rangle\}$ , and a pure quantum state can be written as

$$|\psi\rangle = \sum_j c_j |j\rangle, \quad (1)$$

with complex coefficients  $c_j$  which satisfy  $\sum_j |c_j|^2 = 1$ . The natural choice for free states in the theory of imaginarity are *real states*, i.e., quantum states with all coefficients  $c_j$  being real (up to a non-observable overall phase) [15]. Mixed real states can be identified as convex combinations of real pure states  $|\psi_j\rangle$ ,

$$\rho = \sum_j p_j |\psi_j\rangle\langle\psi_j|. \quad (2)$$

The set of all real states will be denoted by  $\mathcal{R}$ . It can also be characterized as the set of states with a real density matrix [15].

The formulation of a resource theory is completed by defining an appropriate set of free operations, corresponding to physical transformations of the quantum systems which are easy to implement. In general, quantum operations can be specified by a set of Kraus operators  $\{K_j\}$  satisfying the completeness relation  $\sum_j K_j^\dagger K_j = \mathbb{1}$ . In this way, it is guaranteed that  $\Lambda[\rho] = \sum_j K_j \rho K_j^\dagger$  describes a physical transformation,

which can in principle be realized in nature. In the case of probabilistic transformations, the Kraus operators satisfy the more general condition  $\sum_j K_j^\dagger K_j \leq \mathbb{1}$ .

As the free operations of imaginarity theory we identify quantum operations which admit a Kraus decomposition having only real elements in the free basis [15]:

$$\langle m | K_j | n \rangle \in \mathbb{R} \text{ for all } j, m, n. \quad (3)$$

Such transformations are called *real operations* [15]. This definition guarantees that real operations cannot create imaginarity, even if interpreted as a general quantum measurement. In this case, the post-measurement state will be real for any real initial state, regardless of the measurement outcome.

A desirable feature of a quantum resource theory is the existence of a golden unit: a quantum state which can be converted into any other state via free operations. In the resource theory of imaginarity the golden unit is the maximally imaginary state  $|\hat{+}\rangle = (|0\rangle + i|1\rangle)/\sqrt{2}$ . Interestingly, via real operations it is possible to convert  $|\hat{+}\rangle$  into any state of arbitrary dimension [15]. Another maximally imaginary state is given by  $|\hat{-}\rangle = (|0\rangle - i|1\rangle)/\sqrt{2}$ . In the Methods Section we discuss the main features of quantum resource theories, including resource quantifiers and state conversion properties under free operations.

*Quantum state conversion*—We will now present a complete solution for the conversion problem via real operations for all qubit states, characterizing when a qubit state  $\rho$  can be converted into another qubit state  $\sigma$  via real operations. To this end, recall that any single-qubit state can be represented by a real 3-dimensional Bloch vector. Now, the transition  $\rho \rightarrow \sigma$  is possible via real operations if and only if

$$s_y^2 \leq r_y^2, \quad (4a)$$

$$\frac{1 - s_z^2 - s_x^2}{s_y^2} \geq \frac{1 - r_z^2 - r_x^2}{r_y^2}, \quad (4b)$$

where  $\mathbf{r}$  and  $\mathbf{s}$  are the Bloch vectors of the initial and the target state, respectively. A figure illustrating the set of accessible states for different initial states is shown in the Methods Section.

Notably, there exist states  $\sigma$  which cannot be obtained from a given state  $\rho$  via real operations. In this case, it might still be possible to achieve the conversion *probabilistically*. In the following, we present the optimal conversion probability via real operations for any two pure states.

**Theorem 1.** *The maximum probability for a pure state transformation  $|\psi\rangle \rightarrow |\phi\rangle$  via real operations is given by*

$$P(|\psi\rangle \rightarrow |\phi\rangle) = \min \left\{ \frac{1 - |\langle\psi^*|\psi\rangle|}{1 - |\langle\phi^*|\phi\rangle|}, 1 \right\}. \quad (5)$$

The proof of the theorem makes use of properties of general resource quantifiers, we refer to the Methods Section and Supplemental Material for more details.

*Approximate imaginarity distillation*—So far we have discussed *exact* transformations between quantum states via real

operations, both deterministically and stochastically. We will now go one step further, and consider *approximate* transformations, in the cases when an exact transformation is impossible. The figure of merit in this case is the transformation fidelity  $F(\rho \rightarrow \sigma)$ ; we refer to the Methods Section for more details.

Typically, one aims to convert  $\rho$  into the most valuable quantum state, which in the resource theory of imaginarity is the maximally imaginary state  $|\hat{\dagger}\rangle$ . This leads us to the *fidelity of imaginarity*, quantifying the maximal fidelity between a state  $\rho$  and the maximally imaginary state, achievable via real operations:  $F_I(\rho) = F(\rho \rightarrow |\hat{\dagger}\rangle)$ .

As we will see below, the fidelity of imaginarity is closely related to the robustness of imaginarity, defined as [15]

$$\mathcal{I}_R(\rho) = \min_{\tau} \left\{ s > 0 : \frac{\rho + s\tau}{1+s} \in \mathcal{R} \right\}, \quad (6)$$

where  $\tau$  is a (possibly non-real) quantum state. As we show in the Supplemental Material, it admits the following closed formula:  $\mathcal{I}_R(\rho) = \|\rho - \rho^T\|_1/2$ , where  $T$  denotes transposition and  $\|M\|_1 = \text{Tr} \sqrt{M^\dagger M}$  is the trace norm. More details on the robustness measure and its role in general quantum resource theories are given in the Methods Section. Equipped with these tools, we are now ready to give a closed expression for the fidelity of imaginarity.

**Theorem 2.** *For any quantum state  $\rho$  the fidelity of imaginarity is given as*

$$F_I(\rho) = \frac{1 + \mathcal{I}_R(\rho)}{2}. \quad (7)$$

This result provides a closed formula for the fidelity of imaginarity, quantifying how well a quantum state can be converted into the maximally imaginary state  $|\hat{\dagger}\rangle$  via real operations.

*Applications*—We will now discuss applications of imaginarity as a resource for discrimination of quantum states and quantum channels. Channel discrimination can be seen as a game, where one has access to a “black box” with the promise that it implements a quantum channel  $\Lambda_j$  with probability  $p_j$ . The goal of the game is to guess  $\Lambda_j$  by applying the black box to a quantum state  $\rho$ , followed up by a suitably chosen positive operator valued measure (POVM)  $\{M_j\}$  which satisfies  $\sum_j M_j = \mathbb{1}$ ,  $M_j \geq 0$ . The measurement outcome  $j$  then serves as a basis for guessing that the black box has implemented the channel  $\Lambda_j$  in the corresponding realization of the experiment. The probability of correctly guessing an ensemble of channels  $\{p_j, \Lambda_j\}$  in this procedure is given by  $p_{\text{succ}}(\rho, \{p_j, \Lambda_j\}, \{M_j\}) = \sum_j p_j \text{Tr}[M_j \Lambda_j(\rho)]$ .

Recently, it has been shown that *any* quantum resource provides an operational advantage in some channel discrimination task [21, 22]. Specifically, for the resource theory of imaginarity, it holds that

$$\max_{\{p_j, \Lambda_j\}, \{M_j\}} \frac{p_{\text{succ}}(\rho, \{p_j, \Lambda_j\}, \{M_j\})}{\max_{\sigma \in \mathcal{R}} p_{\text{succ}}(\sigma, \{p_j, \Lambda_j\}, \{M_j\})} = 1 + \mathcal{I}_R(\rho). \quad (8)$$

Eq. (8) implies that for any quantum state  $\rho$  which has non-real elements there exists a set of channels such that the optimal guessing probability is strictly larger than for any  $\sigma \in \mathcal{R}$ .

Another, closely related task is *quantum state discrimination* [23], where one aims to distinguish between quantum states  $\rho_j$ , each given with probability  $p_j$ . To this end, one performs quantum measurements, described by a POVM  $\{M_j\}$ . The average probability for correctly guessing the state is  $p_{\text{succ}}(\{p_j, \rho_j\}, \{M_j\}) = \sum_j p_j \text{Tr}[M_j \rho_j]$ . In general, one aims to find a strategy  $\{M_j\}$  which maximizes the success probability for a given ensemble of states and probabilities  $\{p_j, \rho_j\}$ .

To make the role of imaginarity in this task explicit, we extend the robustness of imaginarity from states to measurements. To this end, let  $\mathcal{R}_M$  be the set of all real POVMs  $\{M_j\}$ , i.e., all  $M_j$  have only real elements in the fixed basis. We define the robustness of imaginarity of a measurement  $\{M_j\}$  as

$$\mathcal{I}_R(\{M_j\}) = \min_{\{N_j\}} \left\{ t > 0 : \left\{ \frac{M_j + tN_j}{1+t} \right\} \in \mathcal{R}_M \right\}, \quad (9)$$

where the minimum is taken over all POVMs  $\{N_j\}$ . Following [22], we find a result analogous to Eq. (8):

$$\max_{\{p_j, \rho_j\}} \frac{p_{\text{succ}}(\{p_j, \rho_j\}, \{M_j\})}{\max_{\{F_j\} \in \mathcal{R}_M} p_{\text{succ}}(\{p_j, \rho_j\}, \{F_j\})} = 1 + \mathcal{I}_R(\{M_j\}). \quad (10)$$

For any POVM  $\{M_j\}$  which is outside of  $\mathcal{R}_M$ , there exists an ensemble of states and probabilities  $\{p_j, \rho_j\}$  leading to a better performance of  $\{M_j\}$ , when compared to any measurement with real POVM elements.

Going one step further, we will now show that complex numbers play an indispensable role in *local state discrimination* [10, 24]. Assume that the states to be discriminated are shared by two distant parties, Alice and Bob. It was shown in [25] that any pair of pure orthogonal states can be perfectly distinguished via local operations and classical communication (LOCC). To perfectly distinguish the states  $\{\rho_j^{AB}\}$  via LOCC, there must exist a POVM with elements  $\{M_j\}$  of the form  $M_j = \sum_k A_{j,k} \otimes B_{j,k}$  and the property  $\text{Tr}(M_j \rho_k^{AB}) = \delta_{jk}$  for all  $j$  and  $k$ . If the states  $\{\rho_j^{AB}\}$  are real, we are particularly interested in perfect discrimination with *local real operations and classical communication* (LRCC), where all  $A_{j,k}$ ,  $B_{j,k}$  must be real and symmetric. Indeed, if two states are pure, orthogonal, and real, such perfect LRCC discrimination is possible; see Supplemental Materials for more details.

For some real mixed states, instead, the situation is radically different. Consider the states

$$\begin{aligned} \rho_1^{AB} &= \frac{1}{2} (|\phi^-\rangle\langle\phi^-| + |\psi^+\rangle\langle\psi^+|), \\ \rho_2^{AB} &= \frac{1}{2} (|\phi^+\rangle\langle\phi^+| + |\psi^-\rangle\langle\psi^-|) \end{aligned} \quad (11)$$

with the Bell states  $|\phi^\pm\rangle = (|00\rangle \pm |11\rangle)/\sqrt{2}$ , and  $|\psi^\pm\rangle = (|01\rangle \pm |10\rangle)/\sqrt{2}$ . These states can be perfectly distinguished via LOCC if Alice and Bob perform local measurements in the  $\{|\hat{\dagger}\rangle, |\hat{-}\rangle\}$  basis and share their measurement outcomes via

a classical channel, see Methods Section for more details. On the other hand, the states (11) cannot be distinguished via LRCC with any nonzero probability. To see this, note that the two states can be written as  $\rho_j^{AB} = [\mathbb{1} + (-1)^j \sigma_y \otimes \sigma_y]/4$ , and  $\text{Tr}[S \sigma_y] = 0$  for any real symmetric  $2 \times 2$  matrix  $S$ . It follows that for any POVM element  $M_j = \sum_k A_{j,k} \otimes B_{j,k}$  with real symmetric matrices  $A_{j,k}$  it holds  $\text{Tr}(M_j \rho_1^{AB}) = \text{Tr}(M_j \rho_2^{AB}) = \text{Tr}(M_j)/4$ .

The states (11) show the role of imaginarity for quantum state discrimination in an extreme way. The two states are completely indistinguishable via LRCC, even if we consider imperfect state discrimination with finite error. It is clear from the above discussion that this effect is also observed if only one of the parties is limited to real operations, and the other party has access to all quantum operations locally. Nevertheless, the states can be perfectly distinguished by LOCC, if both Alice and Bob can perform general quantum measurements locally.

These results further highlight the relevance of complex numbers in quantum mechanics. Note that the states (11) have real elements in the computational basis. This means that they are also valid states in ‘‘real quantum theory’’ [1–9], which is the restriction of quantum theory to real states and real measurements. In such a theory, two remote parties would not be able to distinguish these states with any non-zero probability, whereas they are actually perfectly distinguishable in reality.

*Experimental relevance of imaginarity*—Here, we perform a comparison of real operations and general quantum operations in optical experiments, focusing on the single-photon interferometer set-up with half-(quarter-) wave plates and polarizing beam splitters as the building blocks. Moreover, we refer to a wave plate with unset optical axis as unset wave plate. Note that a combination of polarizing beam splitter and half-wave plate plays a similar role as a variable beamsplitter [26–28]. The details of the analysis are given in the Methods Section.

Under above assumptions, a real quantum operation acting on path degree of a  $d$  dimensional system can be implemented with  $(d^6 - d^3)/2$  unset wave plates, whereas a general quantum operation requires at least  $d^6 - 1$  unset wave plates for the implementation. We assume that both operations are implemented via a unitary dilation, see Methods Section for more details. For large  $d$ , this implementation allows one to reduce the number of unset wave plates by a factor of 1/2, if real operations are used instead of general quantum operations.

Similar results can be found in implementing a real  $n$ -outcome generalized measurement on a single polarization-encoded qubit [29], when compared to the corresponding general qubit measurement. Even in this case, using real measurements instead of general measurements reduces the number of unset wave plates by 1/2 in the limit of large  $n$ .

These results show that real states are easier to create and real operations are easier to perform when compared to general states and operations in a single-photon interferometer set-up. This justifies the choice of real states (operations) as the free states (operations) of the resource theory of imaginarity.

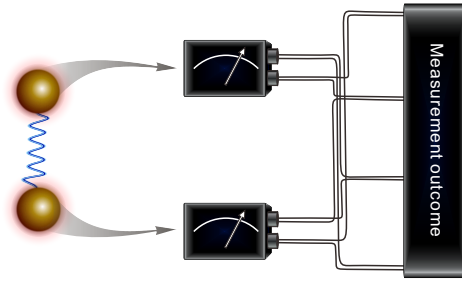


FIG. 1. **Experimental protocol.** The experiments are carried out using linear optics. We prepare entangled photon sources and perform local projective measurements on each photon, identifying the successful guessing probability by classical communications.

*Experimental local state discrimination*—As discussed earlier, imaginarity plays an important role for quantum state discrimination. We devised an experimental setup for local state discrimination using two entangled photons. The experimental protocol and setup are shown in Fig. 1. Our setup allows us to prepare a class of two-qubit states, and determine the optimal guessing probability under LOCC.

Our experiment consists of two parts. In the first part we consider the discrimination of the two states in Eq. (11). We recall that these states can be perfectly distinguished if Alice and Bob perform local projective measurements in the maximally imaginary basis  $\{| \hat{\rangle}, | \hat{\langle} \rangle\}$  and share the outcomes of their measurement via a classical channel. The experimental results are shown in Fig. 2 (a). From the experimental data we obtain  $P = 0.984$  for the success probability [30–32]. To demonstrate that the states cannot be distinguished if the local measurements are real, we also show the experimentally measured probabilities of the  $\sigma_x$  and  $\sigma_z$  measurements. In this case the output is nearly a uniform distribution. From the right side of Fig. 2 (a), we extract experimentally determined guessing probabilities under different local Pauli measurements and classical communications. We can see that imaginarity is necessary in measurement of both subsystems for improving the guessing probability, since any real projective measurements can be written as a combination of  $\mathbb{1}$ ,  $\sigma_x$ , and  $\sigma_z$ .

In Fig. 2 (b–e), we show the experimental results for distinguishing different families of mixed states. The exact expression for the states is given in the caption of Fig. 2. All dashed lines represent theoretically derived maximum probability for distinguishing the states via local projective measurement and classical communication; dotted lines represent the aforementioned probabilities under local *real* measurements, we refer to the caption of Fig. 2 and the Supplemental Material for more details. Note that all states considered here have only real elements in the computational basis.

These results clearly demonstrate the relevance of imaginarity to local state discrimination. The ability to perform measurements with non-real POVM elements can significantly improve the success probability for state discrimination, even if the states to be distinguished have real density matrices.

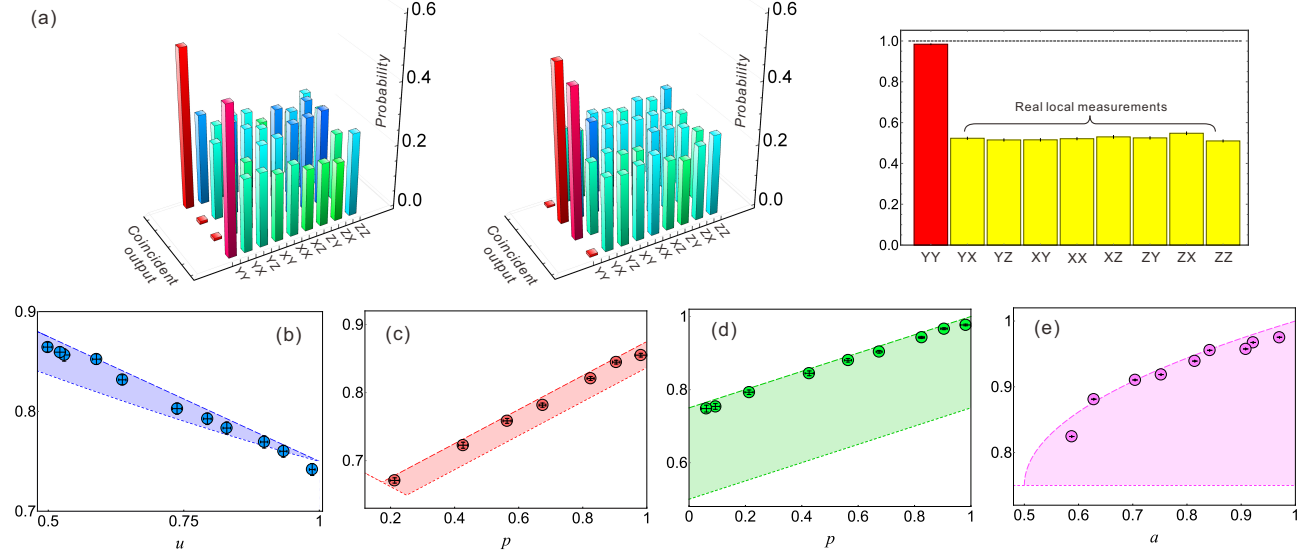


**FIG. 2. Experimental results for local state discrimination.** All discrimination tasks concern output states after some local free operations, when the initial state is prepared as a Bell state. In (a) we present the probabilities for the extreme examples in Eq. (11), in the standard local Pauli measurements. The right part of (a) shows the experimentally measured guessing probabilities under different strategies. In (b-e), we present the experimental results for the local discrimination of different families of real bipartite states. The families of states are defined as follows: (b)  $|\phi^+\rangle\langle\phi^+|$ , and  $[\psi_0|\phi^+\rangle\langle\phi^+| + (1-\psi_0)|\phi^-\rangle\langle\phi^-| + |\psi_1|\phi^+\rangle\langle\phi^-| + (1-\psi_1)|\phi^-\rangle\langle\phi^+|]/2$ , where  $|\psi\rangle = \psi_{00}|00\rangle + \psi_{01}|01\rangle + \psi_{10}|10\rangle + \psi_{11}|11\rangle$  is a non-trivial entangled pure state with  $\psi_{00} = -\psi_{11} \approx 0.54$  and  $\psi_{01} = \psi_{10} \approx 0.46$ ; (c)  $p|\phi^+\rangle\langle\phi^+| + (1-p)|\phi^-\rangle\langle\phi^-|/4$  and  $(|\phi^+\rangle\langle\phi^+| + |\phi^-\rangle\langle\phi^-| + 2|\psi\rangle\langle\psi|)/4$ ; (d)  $(|\phi^-\rangle\langle\phi^-| + |\psi^+\rangle\langle\psi^+|)/2$  and  $p|\phi^+\rangle\langle\phi^+| + (1-p)|\phi^-\rangle\langle\phi^-|/4$ ; (e)  $\frac{1}{2}(|\phi^-\rangle\langle\phi^-| + |\psi^+\rangle\langle\psi^+|)$  and a class of maximally correlated mixed states, with  $a$  denoting their purity. Dashed and dotted lines represent theoretical bounds for guessing probabilities using complex measurements and real measurements, respectively. The shaded areas represent the advantage of using complex measurements over real ones. We refer to the Supplemental Material for more details.

## DISCUSSION

In this work, we investigate the resource theory of imaginarity, studying the role of complex numbers in quantum mechanics in an operational way. We formulate and completely solve several questions within this theory, including the deterministic conversion for all qubit states, the probabilistic conversion for all pure states, and the single-shot imaginarity distillation for all states of arbitrary dimension.

Our methods can be readily applied to study the role of complex number in quantum information processing tasks. We demonstrate this for local state discrimination, where two remote parties aim to distinguish states by applying local operations and classical communication. We show – both theoretically and experimentally – that there exist real quantum states which can be perfectly distinguished in this setup if imaginarity is used in the local measurements. However, when restricting to only real measurements, the states cannot be distinguished with any nonzero probability. This demonstrates that complex numbers are an essential ingredient of quantum mechanics.

The usefulness of complex number in quantum mechanics is worth an in-depth study also in the light of the recent advances in quantum technologies. An important example is quantum computers, which can solve certain problems of interest significantly faster than any classical computer [33, 34]. As of today, the reason for this quantum advantage is not com-

pletely understood, especially when it comes to quantum computers operating on noisy states [35–39]. A quantitative analysis of imaginarity in quantum computers can shed new light on the quantum features required for the quantum speedup. Another promising line of research is the relation between different quantum resources [40–44], which will give us new insights into quantum resource consumption in quantum technological tasks, such as quantum metrology and quantum communication.

## METHODS

### Main features of quantum resource theories

One of the main questions in any quantum resource theory is whether for two given quantum states  $\rho$  and  $\sigma$  there exists a free operation  $\Lambda_f$  transforming  $\rho$  into  $\sigma$ :

$$\sigma = \Lambda_f[\rho]. \quad (12)$$

The existence of such a transformation immediately implies that  $\rho$  is more resourceful than  $\sigma$ , and in particular

$$R(\rho) \geq R(\sigma) \quad (13)$$

for any resource measure  $R$ .

If  $\rho$  cannot be converted into  $\sigma$  via a free operation, e.g. if  $R(\rho) < R(\sigma)$ , it might still be possible to achieve the conversion probabilistically, if the corresponding resource theory allows for stochastic free operations, with free Kraus operators  $\{K_j\}$  such that  $\sum_i K_j^\dagger K_j \leq \mathbb{1}$ . The maximal probability for converting  $\rho$  into  $\sigma$  is then defined as

$$P(\rho \rightarrow \sigma) = \max \left\{ \sum_j p_j : \sigma = \frac{\sum_j K_j \rho K_j^\dagger}{\sum_j p_j} \right\} \quad (14)$$

with probabilities  $p_j = \text{Tr}[K_j \rho K_j^\dagger]$ , and the maximum is taken over all (possibly incomplete) sets of free Kraus operators, i.e.,  $\sum_i K_i^\dagger K_i \leq \mathbb{1}$ . The existence of a deterministic free operation between  $\rho$  and  $\sigma$  as in Eq. (12) is then equivalent to  $P(\rho \rightarrow \sigma) = 1$ .

If two states  $\rho$  and  $\sigma$  do not allow for deterministic neither stochastic transformations [i.e.,  $P(\rho \rightarrow \sigma) = 0$ ], there remains the possibility to perform the transformation approximately. The figure of merit in this case is the maximal transformation fidelity

$$F(\rho \rightarrow \sigma) = \max_{\Lambda_f} \{F(\Lambda_f[\rho], \sigma)\}, \quad (15)$$

with fidelity  $F(\rho, \sigma) = \left( \text{Tr} \sqrt{\sqrt{\rho} \sigma \sqrt{\rho}} \right)^2$ , and the maximum is taken over all free operations  $\Lambda_f$ .

Any resource measure  $R$  is monotonic under free operations, see Eq. (13). For resource theories which allow for stochastic conversion, one typically requires a stronger constraint on the resource measure, to be monotonic on average under free operations:

$$R(\rho) \geq \sum_j q_j R(\sigma_j). \quad (16)$$

Here, the states  $\sigma_j$  arise from  $\rho$  by applying a free operation:  $\sigma_j = K_j \rho K_j^\dagger / q_j$  with free Kraus operators  $K_j$ , and  $q_j$  is the corresponding probability:  $q_j = \text{Tr}[K_j \rho K_j^\dagger]$ . Quantifiers satisfying Eq. (16) are also called *strong resource monotones*. If  $R$  is additionally convex, i.e.,  $R(\sum_j p_j \rho_j) \leq \sum_j p_j R(\rho_j)$ , then strong monotonicity (16) implies the weaker condition (13).

A powerful upper bound on the conversion probability (14) can be obtained from any resource quantifier which is convex and strongly monotonic under free operations. For any such resource quantifier  $R$ , it holds [45]:

$$P(\rho \rightarrow \sigma) \leq \min \left\{ \frac{R(\rho)}{R(\sigma)}, 1 \right\}. \quad (17)$$

An important resource quantifier is the robustness with respect to set of free states  $\mathcal{F}$ :

$$R_{\mathcal{F}}(\rho) = \min_{\tau} \left\{ s > 0 : \frac{\rho + s\tau}{1+s} \in \mathcal{F} \right\}, \quad (18)$$

where the minimum is taken over all quantum states  $\tau$ . For any quantum resource theory, the robustness is closely related

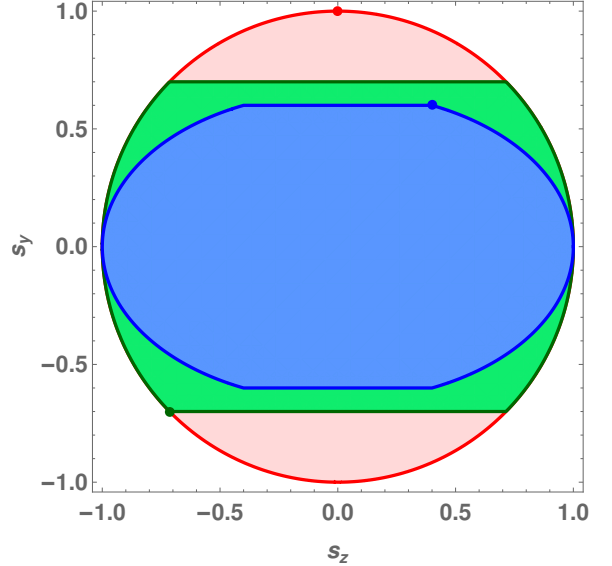


FIG. 3. **State transformation via real operations for qubit systems.** The plot shows the  $y$ - $z$  projections of accessible states for initial qubit states with Bloch vectors  $(0, 0.6, 0.4)$  [blue dot],  $(0, -0.7, -\sqrt{0.51})$  [green dot], and  $(0, 1, 0)$  [red dot]. Note that the second and third states are pure. The corresponding accessible area in the  $y$ - $z$  plane is shown in blue, green, and red, respectively. The full accessible area is obtained by rotation around the  $y$ -axis.

to the success probability in channel discrimination tasks [21, 22]:

$$\max_{\{p_j, \Lambda_j\}, \{M_j\}} \frac{p_{\text{succ}}(\rho, \{p_j, \Lambda_j\}, \{M_j\})}{\max_{\sigma \in \mathcal{F}} p_{\text{succ}}(\sigma, \{p_j, \Lambda_j\}, \{M_j\})} = 1 + R_{\mathcal{F}}(\rho). \quad (19)$$

Eq. (19) implies that for any resource state  $\rho$  (i.e. a quantum state which is not element of  $\mathcal{F}$ ) there exist a set of channels  $\{\Lambda_j\}$  and a probability distribution  $\{p_j\}$  such that the optimal guessing probability is strictly larger than for any  $\sigma \in \mathcal{F}$ .

### State transformations via real operations

For single-qubit states, possible transformations via real operations are fully characterized by Eqs. (4). The proof of this result makes use of methods developed earlier within the resource theory of quantum coherence [46–48], and more details can be found in the Supplemental Material. In Fig. 3 we show the  $y$ - $z$ -projection of the accessible region for three different initial states. The complete region can be obtained by rotation around the  $y$ -axis.

The proof of Theorem 1 for probabilistic conversion of pure states makes use of properties of resource monotones and their relation to conversion probability in Eq. (17). We refer to Supplemental Materials for more details.

## Role of real operations in optical experiments

In standard linear optics using the polarization and path degrees of freedom of photons, real operations can be implemented more economically, compared to general quantum operations. We begin with a simple observation, that implementing a general unitary on photon polarization requires to control at least 3 wave plates (this is due to a qubit unitary being specified by 3 parameters), whereas only one half-wave plate is needed if the unitary has only real components, e.g., rotation about the  $y$ -axis. As pointed out before, when restricting the optical elements to half (quarter)-wave plates, a rotation about the  $z$ -axis needs two additional quarter-wave plates compared to a rotation about the  $y$ -axis. This observation is the first evidence that the set of real operations is potentially easier to implement in terms of the number of optical elements, compared to the set of complex quantum operations.

We then consider single-qubit measurement with  $n$  outcomes. As illustrated in Fig. 4, any such measurement can be implemented with  $8n - 5$  unset wave plates. If  $n = 2$ , we have two Kraus operators  $K_0$  and  $K_1$  with

$$K_1^\dagger K_1 = \mathbb{1} - K_0^\dagger K_0. \quad (20)$$

By singular value decomposition, there are unitaries  $U_i$  and  $V_i$  such that  $K_j = U_j S_j V_j$ , and  $S_j$  are diagonal matrices with nonnegative entries. By Eq. (20) we obtain

$$V_1^\dagger S_1^2 V_1 = V_0^\dagger (\mathbb{1} - S_0^2) V_0, \quad (21)$$

which implies that  $V_0 = V_1$  and  $S_1 = (\mathbb{1} - S_0^2)^{1/2}$ . In summary, a general two-outcome measurement can be performed by applying a unitary  $V_0$ , followed by a two-outcome measurement with diagonal Kraus operators  $S_0$  and  $S_1$ , and — depending on the measurement outcome — completed by a conditional unitary  $U_0$  or  $U_1$ . A setup realizing this procedure on photon polarization is shown in Fig. 4. The unitaries  $V_0$ ,  $U_0$ , and  $U_1$  on the polarization-encoded qubit can be realized by 3 wave plates per unitary, while the measurement with diagonal Kraus operators  $\{S_0, S_1\}$  can be realized with 3 beam displacers and 5 wave plates, of which 2 are unset. This amounts to 11 unset wave plates in total. By using the same procedure repeatedly, this setup can be extended to  $n$  Kraus operators, see also [49]. For each additional Kraus operator we need 8 unset wave plates, giving  $8n - 5$  unset wave plates in total, as claimed.

If all Kraus operators are real, fewer wave plates are needed. This can be seen from the fact that the singular value decomposition of each  $K_j$  can be done with real  $U_j$  and  $V_j$ . Thus, a real measurement with two outcomes can be implemented with 5 unset wave plates, and each additional real Kraus operator requires 4 additional wave plates, see also Fig. 4. The number  $4n - 3$  is optimal, since it corresponds to the number of independent real parameters for  $n$  real Kraus operators. Compared to  $8n - 5$  unset wave plates for a general  $n$ -outcome measurement via the method presented above, in the limit  $n \rightarrow \infty$  we can save approximately half of the optical elements if we restrict ourselves to real measurements.

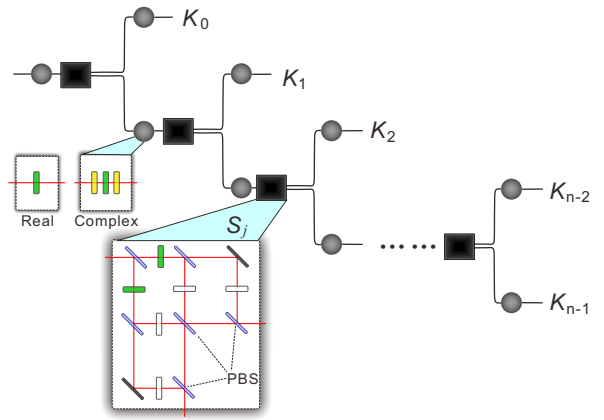


FIG. 4. **Linear optical implementation of real and general qubit operations with polarized photons.** Green and yellow plates represent unset wave plates (WP), while gray ones represent fixed wave plates that we don't need to control. Thin strips denote beam splitters which can separate the horizontally polarized photons from vertically polarized ones. Round nodes represent orthogonal or unitary operations, and boxes represent the operations  $S_j$ , which have two outcomes. For general real operations we only need to control half-wave plates, while for complex ones we have to add quarter-wave plates for manipulating the imaginary part of the photonic states.

For implementing a real operation of arbitrary dimension, fewer optical elements are needed compared with the corresponding number for a general quantum operation, due to the upper bound of number of parameters to specify these operations. Note that every real operation acting on a system of dimension  $d$  has a real dilation [15]:

$$\Lambda_{\text{RO}}^A[\rho^A] = \text{Tr}_B \left[ O_{AB} \left( \rho^A \otimes |0\rangle\langle 0|^B \right) O_{AB}^T \right], \quad (22)$$

where  $O_{AB}$  is a  $d^3 \times d^3$  real orthogonal matrix. Correspondingly, a general quantum operation admits a dilation with a general  $d^3 \times d^3$  unitary matrix. Implementing an  $m \times m$  unitary in path degree requires at least  $m^2 - 1$  unset wave plates, corresponding to the number of real parameters of the unitary. On the other hand, a real orthogonal matrix can be decomposed into  $(m^2 - m)/2$  real orthogonal matrices, each acting on two levels. Since a real orthogonal two-level matrix can be implemented with a single wave plate, any real orthogonal  $m \times m$  matrix can be implemented by using  $(m^2 - m)/2$  unset wave plates. Thus, implementing a real operation can be achieved with  $(d^6 - d^3)/2$  unset wave plates. Instead, implementing a general quantum operation in the same way requires at least  $d^6 - 1$  unset wave plates. For large  $d$ , restricting ourselves to real operations reduces the number of unset wave plates by  $1/2$ , when compared to the number of wave plates for a general quantum operations implemented via a unitary dilation.

## Imaginarity in local state discrimination

For two mixed states  $\rho_1^{AB}$  and  $\rho_2^{AB}$  to be perfectly distinguishable via LOCC, there must exist a POVM with elements

$\{M_1, M_2\}$  of the form

$$M_j = \sum_k A_{j,k} \otimes B_{j,k} \quad (23)$$

with Hermitian  $A_{j,k}$  and  $B_{j,k}$ , and moreover

$$\text{Tr} [M_1 \rho_1^{AB}] = \text{Tr} [M_2 \rho_2^{AB}] = 1, \quad (24a)$$

$$\text{Tr} [M_1 \rho_2^{AB}] = \text{Tr} [M_2 \rho_1^{AB}] = 0. \quad (24b)$$

Correspondingly, if the states are distinguishable via LRCC,  $A_{j,k}$  and  $B_{j,k}$  must be real and symmetric.

The states in Eq. (11) are distinguishable via LOCC if Alice and Bob perform local measurements in the  $\{|\hat{+}\rangle, |\hat{-}\rangle\}$  basis and share their measurement outcomes via a classical channel. The corresponding POVM elements are given as

$$M_1 = |\hat{+}\rangle\langle\hat{+}| \otimes |\hat{+}\rangle\langle\hat{+}| + |\hat{-}\rangle\langle\hat{-}| \otimes |\hat{-}\rangle\langle\hat{-}|, \quad (25a)$$

$$M_2 = |\hat{+}\rangle\langle\hat{+}| \otimes |\hat{-}\rangle\langle\hat{-}| + |\hat{-}\rangle\langle\hat{-}| \otimes |\hat{+}\rangle\langle\hat{+}|. \quad (25b)$$

We verify that Eqs. (24) are satisfied, implying that this POVM perfectly discriminates the states (11). As is explained in the main text, the states (11) cannot be discriminated via LRCC with any non-zero probability.

## ACKNOWLEDGMENTS

T.V.K., S.R., and A.S. acknowledge financial support by the “Quantum Optical Technologies” project, carried out within the International Research Agendas programme of the Foundation for Polish Science co-financed by the European Union under the European Regional Development Fund. C.M.S. acknowledges the hospitality of the Centre for Quantum Optical Technologies at the University of Warsaw, and financial support by the Pacific Institute for the Mathematical Sciences (PIMS) and a Faculty of Science Grand Challenge award at the University of Calgary.

---

[1] E. C. Stückelberg, Quantum theory in real Hilbert space, *Helv. Phys. Acta* **33**, 458 (1960).

[2] H. Araki, On a characterization of the state space of quantum mechanics, *Commun. Math. Phys.* **75**, 1 (1980).

[3] L. Hardy and W. K. Wootters, Limited holism and real-vector-space quantum theory, *Found. Phys.* **42**, 454 (2012).

[4] W. K. Wootters, Entanglement sharing in real-vector-space quantum theory, *Found. Phys.* **42**, 19 (2012).

[5] J. C. Baez, Division algebras and quantum theory, *Found. Phys.* **42**, 819 (2012).

[6] A. Aleksandrova, V. Borish, and W. K. Wootters, Real-vector-space quantum theory with a universal quantum bit, *Phys. Rev. A* **87**, 052106 (2013).

[7] W. K. Wootters, The rebit three-tangle and its relation to two-qubit entanglement, *J. Phys. A* **47**, 424037 (2014).

[8] W. K. Wootters, Optimal information transfer and real-vector-space quantum theory, in *Quantum Theory: Informational Foundations and Foils*, edited by G. Chiribella and R. W. Spekkens (Springer Netherlands, Dordrecht, 2016) pp. 21–43.

[9] H. Barnum, M. A. Graydon, and A. Wilce, Composites and categories of Euclidean Jordan algebras, [arXiv:1606.09331 \[quant-ph\]](https://arxiv.org/abs/1606.09331) (2016).

[10] W. K. Wootters, Local accessibility of quantum states, in *Complexity, Entropy and the Physics of Information*, edited by W. H. Zurek (Addison-Wesley, 1990) pp. 39–46.

[11] Q. Liu, T. J. Elliott, F. C. Binder, C. Di Franco, and M. Gu, Optimal stochastic modeling with unitary quantum dynamics, *Phys. Rev. A* **99**, 062110 (2019).

[12] M. Horodecki and J. Oppenheim, (Quantumness in the context of) resource theories, *Int. J. Mod. Phys. B* **27**, 1345019 (2013).

[13] F. G. S. L. Brandão and G. Gour, Reversible framework for quantum resource theories, *Phys. Rev. Lett.* **115**, 070503 (2015).

[14] E. Chitambar and G. Gour, Quantum resource theories, *Rev. Mod. Phys.* **91**, 025001 (2019).

[15] A. Hickey and G. Gour, Quantifying the imaginarity of quantum mechanics, *J. Phys. A* **51**, 414009 (2018).

[16] R. Horodecki, P. Horodecki, M. Horodecki, and K. Horodecki, Quantum entanglement, *Rev. Mod. Phys.* **81**, 865 (2009).

[17] A. Streltsov, G. Adesso, and M. B. Plenio, Colloquium: Quantum coherence as a resource, *Rev. Mod. Phys.* **89**, 041003 (2017).

[18] J. Goold, M. Huber, A. Riera, L. del Rio, and P. Skrzypczyk, The role of quantum information in thermodynamics—a topical review, *J. Phys. A* **49**, 143001 (2016).

[19] M. Lostaglio, An introductory review of the resource theory approach to thermodynamics, *Rep. Prog. Phys.* **82**, 114001 (2019).

[20] T. Baumgratz, M. Cramer, and M. B. Plenio, Quantifying coherence, *Phys. Rev. Lett.* **113**, 140401 (2014).

[21] R. Takagi, B. Regula, K. Bu, Z.-W. Liu, and G. Adesso, Operational advantage of quantum resources in subchannel discrimination, *Phys. Rev. Lett.* **122**, 140402 (2019).

[22] R. Takagi and B. Regula, General resource theories in quantum mechanics and beyond: Operational characterization via discrimination tasks, *Phys. Rev. X* **9**, 031053 (2019).

[23] A.Chefles, Quantum state discrimination, *Contemporary Physics* **41**, 401 (2000).

[24] S. Bergia, F. Cannata, A. Cornia, and R. Livi, On the actual measurability of the density matrix of a decaying system by means of measurements on the decay products, *Found. Phys.* **10**, 723 (1980).

[25] J. Walgate, A. J. Short, L. Hardy, and V. Vedral, Local distinguishability of multipartite orthogonal quantum states, *Phys. Rev. Lett.* **85**, 4972 (2000).

[26] M. Reck, A. Zeilinger, H. J. Bernstein, and P. Bertani, Experimental realization of any discrete unitary operator, *Physical review letters* **73**, 58 (1994).

[27] P. Kok, W. J. Munro, K. Nemoto, T. C. Ralph, J. P. Dowling, and G. J. Milburn, Linear optical quantum computing with photonic qubits, *Reviews of Modern Physics* **79**, 135 (2007).

[28] J. Carolan, C. Harrold, C. Sparrow, E. Martín-López, N. J. Russell, J. W. Silverstone, P. J. Shadbolt, N. Matsuda, M. Oguma, M. Itoh, *et al.*, Universal linear optics, *Science* **349**, 711 (2015).

[29] Y.-y. Zhao, N.-k. Yu, P. Kurzyński, G.-y. Xiang, C.-F. Li, and G.-C. Guo, Experimental realization of generalized qubit measurements based on quantum walks, *Physical Review A* **91**, 042101 (2015).

[30] R. B. Clarke, A. Chefles, S. M. Barnett, and E. Riis, Experimental demonstration of optimal unambiguous state discrimination, *Physical Review A* **63**, 040305 (2001).

[31] P. J. Mosley, S. Croke, I. A. Walmsley, and S. M. Barnett, Experimental realization of maximum confidence quantum state discrimination for the extraction of quantum information, *Physical review letters* **97**, 193601 (2006).

[32] M. Solís-Prosser, M. Fernandes, O. Jiménez, A. Delgado, and L. Neves, Experimental minimum-error quantum-state discrimination in high dimensions, *Physical Review Letters* **118**, 100501 (2017).

[33] S. Bravyi, D. Gosset, and R. König, Quantum advantage with shallow circuits, *Science* **362**, 308 (2018).

[34] F. Arute, K. Arya, R. Babbush, D. Bacon, J. C. Bardin, R. Barends, R. Biswas, S. Boixo, F. G. S. L. Brandao, D. A. Buell, B. Burkett, Y. Chen, Z. Chen, B. Chiaro, R. Collins, W. Courtney, A. Dunsworth, E. Farhi, B. Foxen, A. Fowler, C. Gidney, M. Giustina, R. Graff, K. Guerin, S. Habegger, M. P. Harrigan, M. J. Hartmann, A. Ho, M. Hoffmann, T. Huang, T. S. Humble, S. V. Isakov, E. Jeffrey, Z. Jiang, D. Kafri, K. Kechedzhi, J. Kelly, P. V. Klimov, S. Knysh, A. Korotkov, F. Kostritsa, D. Landhuis, M. Lindmark, E. Lucero, D. Lyakh, S. Mandrà, J. R. McClean, M. McEwen, A. Megrant, X. Mi, K. Michelsen, M. Mohseni, J. Mutus, O. Naaman, M. Neeley, C. Neill, M. Y. Niu, E. Ostby, A. Petukhov, J. C. Platt, C. Quintana, E. G. Rieffel, P. Roushan, N. C. Rubin, D. Sank, K. J. Satzinger, V. Smelyanskiy, K. J. Sung, M. D. Trevithick, A. Vainsencher, B. Villalonga, T. White, Z. J. Yao, P. Yeh, A. Zalcman, H. Neven, and J. M. Martinis, Quantum supremacy using a programmable superconducting processor, *Nature* **574**, 505 (2019).

[35] E. Knill and R. Laflamme, Power of one bit of quantum information, *Phys. Rev. Lett.* **81**, 5672 (1998).

[36] A. Datta, S. T. Flammia, and C. M. Caves, Entanglement and the power of one qubit, *Phys. Rev. A* **72**, 042316 (2005).

[37] A. Datta, A. Shaji, and C. M. Caves, Quantum discord and the power of one qubit, *Phys. Rev. Lett.* **100**, 050502 (2008).

[38] B. Dakić, V. Vedral, and Č. Brukner, Necessary and sufficient condition for nonzero quantum discord, *Phys. Rev. Lett.* **105**, 190502 (2010).

[39] J. M. Matera, D. Egloff, N. Killoran, and M. B. Plenio, Coherent control of quantum systems as a resource theory, *Quantum Sci. Technol.* **1**, 01LT01 (2016).

[40] A. Streltsov, U. Singh, H. S. Dhar, M. N. Bera, and G. Adesso, Measuring quantum coherence with entanglement, *Phys. Rev. Lett.* **115**, 020403 (2015).

[41] J. Ma, B. Yadin, D. Girolami, V. Vedral, and M. Gu, Converting coherence to quantum correlations, *Phys. Rev. Lett.* **116**, 160407 (2016).

[42] K.-D. Wu, Z. Hou, Y.-Y. Zhao, G.-Y. Xiang, C.-F. Li, G.-C. Guo, J. Ma, Q.-Y. He, J. Thompson, and M. Gu, Experimental cyclic interconversion between coherence and quantum correlations, *Phys. Rev. Lett.* **121**, 050401 (2018).

[43] W. Wang, J. Han, B. Yadin, Y. Ma, J. Ma, W. Cai, Y. Xu, L. Hu, H. Wang, Y. P. Song, M. Gu, and L. Sun, Witnessing quantum resource conversion within deterministic quantum computation using one pure superconducting qubit, *Phys. Rev. Lett.* **123**, 220501 (2019).

[44] C. Sparaciari, L. del Rio, C. M. Scandolo, P. Faist, and J. Oppenheim, The first law of general quantum resource theories, *Quantum* **4**, 259 (2020).

[45] K.-D. Wu, T. Theurer, G.-Y. Xiang, C.-F. Li, G.-C. Guo, M. B. Plenio, and A. Streltsov, Quantum coherence and state conversion: theory and experiment, *npj Quantum Inf.* **6**, 22 (2020).

[46] A. Streltsov, S. Rana, P. Boes, and J. Eisert, Structure of the resource theory of quantum coherence, *Phys. Rev. Lett.* **119**, 140402 (2017).

[47] E. Chitambar and G. Gour, Critical examination of incoherent operations and a physically consistent resource theory of quantum coherence, *Phys. Rev. Lett.* **117**, 030401 (2016).

[48] E. Chitambar and G. Gour, Comparison of incoherent operations and measures of coherence, *Phys. Rev. A* **94**, 052336 (2016).

[49] S. E. Ahnert and M. C. Payne, General implementation of all possible positive-operator-value measurements of single-photon polarization states, *Phys. Rev. A* **71**, 012330 (2005).

[50] J. Aberg, Quantifying Superposition, *arXiv:quant-ph/0612146* (2006).

[51] R. A. Horn and C. R. Johnson, *Matrix Analysis*, 2nd ed. (Cambridge University Press, 2012).

[52] M. A. Nielsen and I. L. Chuang, *Quantum Computation and Quantum Information*, 10th ed. (Cambridge University Press, USA, 2010).

[53] K.-D. Wu, Z. Hou, H.-S. Zhong, Y. Yuan, G.-Y. Xiang, C.-F. Li, and G.-C. Guo, Experimentally obtaining maximal coherence via assisted distillation process, *Optica* **4**, 454 (2017).

[54] B. Qi, Z. Hou, Y. Wang, D. Dong, H.-S. Zhong, L. Li, G.-Y. Xiang, H. M. Wiseman, C.-F. Li, and G.-C. Guo, Adaptive quantum state tomography via linear regression estimation: Theory and two-qubit experiment, *npj Quantum Inf.* **3**, 19 (2017).

## SUPPLEMENTAL MATERIAL

### A. Proof of Eqs. (4)

Here we will study deterministic state conversion via real operations, resorting to the large amount of tools developed within the resource theory of coherence [17]. To use this analogy in an optimal way, we introduce a new set of operations, which we term *y-z-preserving operations* and denote by  $\Lambda_{yz}$ . They correspond to single-qubit quantum operations which map the *y-z* plane of the Bloch space onto itself, i.e., if a state  $\rho$  has a Bloch vector in the *y-z* plane, then  $\Lambda_{yz}[\rho]$  also has this property. In the same way, *x-z*-preserving operations map the set of real states onto itself. Similarly, *z*-preserving operations map diagonal states onto diagonal states, thus corresponding to maximally incoherent operations (MIO) [50].

In the following we will prove two lemmas, thus demonstrating a close relation between the resource theories of coherence and imaginarity.

**Lemma 1.** *Let  $\rho_r$  and  $\sigma_r$  be qubit states with Bloch vectors in the *x-z* plane. If there exists a *y-z*-preserving operation  $\Lambda_{yz}$  such that  $\Lambda_{yz}[\rho_r] = \sigma_r$ , there also exists a *z*-preserving operation  $\Lambda_z$  such that  $\Lambda_z[\rho_r] = \sigma_r$ .*

*Proof.* Since  $\Lambda_{yz}$  is *y-z* preserving, it converts both states  $|0\rangle$  and  $|1\rangle$  into states  $\mu_0$  and  $\mu_1$  with Bloch vectors in the *y-z* plane, i.e.,  $\mu_0$  and  $\mu_1$  have purely imaginary off-diagonal elements. This implies that any convex combination of  $|0\rangle$  and  $|1\rangle$  is also converted into a state with purely imaginary off-diagonal elements.

Let now  $\{K_j\}$  be the Kraus operators of  $\Lambda_{yz}$ . We introduce another transformation

$$\Lambda'(\rho) = \sum_j L_j \rho L_j^\dagger \quad (26)$$

with Kraus operators  $L_j = K_j^*$ . It is straightforward to verify that  $\{L_j\}$  is indeed a valid set of Kraus operators:

$$\sum_j L_j^\dagger L_j = \sum_j (K_j^*)^\dagger K_j^* = \sum_j K_j^T K_j^* = \sum_j (K_j^\dagger K_j)^* = \mathbb{1}. \quad (27)$$

Moreover, when applied to any state  $\tau_r$  in the *x-z* plane, we obtain

$$\Lambda'(\tau_r) = \sum_j K_j^* \tau_r K_j^T = \left( \sum_j K_j \tau_r K_j^\dagger \right)^* = \left[ \Lambda_{yz}(\tau_r) \right]^T, \quad (28)$$

where in the last step we used the fact that  $\Lambda_{yz}(\tau_r)$  is Hermitian. It follows that

$$\Lambda'[\rho_r] = \sigma_r, \quad (29a)$$

$$\Lambda' [|0\rangle\langle 0|] = \mu_0^T, \quad (29b)$$

$$\Lambda' [|1\rangle\langle 1|] = \mu_1^T. \quad (29c)$$

In the next step, we introduce the transformation

$$\tilde{\Lambda}(\rho) = \frac{1}{2} \Lambda_{yz}(\rho) + \frac{1}{2} \Lambda'(\rho). \quad (30)$$

Recalling that the states  $\mu_0$  and  $\mu_1$  have purely imaginary off-diagonal elements, we further obtain

$$\tilde{\Lambda}[\rho_r] = \sigma_r, \quad (31a)$$

$$\tilde{\Lambda}[|0\rangle\langle 0|] = \frac{1}{2} (\mu_0 + \mu_0^T) = \sum_j \langle j | \mu_0 | j \rangle | j \rangle \langle j |, \quad (31b)$$

$$\tilde{\Lambda}[|1\rangle\langle 1|] = \frac{1}{2} (\mu_1 + \mu_1^T) = \sum_j \langle j | \mu_1 | j \rangle | j \rangle \langle j |. \quad (31c)$$

This implies that  $\tilde{\Lambda}$  is a *z*-preserving operation transforming  $\rho_r$  onto  $\sigma_r$ .  $\square$

In the next step, we will use Lemma 1 to characterize the set of real states achievable from a given real state  $\rho$  via *y-z*-preserving operations.

**Lemma 2.** *Let  $\rho_r$  and  $\sigma_r$  be qubit states in the *x-z* plane of the Bloch sphere. Then, there exists a *y-z*-preserving operation such that  $\sigma_r = \Lambda_{yz}[\rho_r]$  if and only if*

$$s_x^2 \leq r_x^2, \quad (32)$$

$$\frac{1 - s_z^2}{s_x^2} \geq \frac{1 - r_z^2}{r_x^2}, \quad (33)$$

where  $\mathbf{r}$  and  $\mathbf{s}$  denote the Bloch vectors of  $\rho_r$  and  $\sigma_r$ , respectively.

*Proof.* We will first prove that a *y-z*-preserving operation violating Eq. (32) and/or Eq. (33) does not exist. Assume – by contradiction – that there exists a *y-z*-preserving operation violating Eq. (32) and/or Eq. (33). Then, by Lemma 1 there must also exist a *z*-preserving (i.e. MIO) operation such that  $\sigma_r = \Lambda_{MIO}[\rho_r]$ . Such a transformation does not exist due to results in [46–48].

We will now show that a *y-z*-preserving operation exists if Eqs. (32) and (33) are fulfilled. Note that  $\sigma_z$  and any rotation around the *x*-axis are *y-z*-preserving operations. Thus, we can restrict ourselves to the positive part of the Bloch space, i.e., all Bloch coordinates considered in the following are non-negative. Moreover, we are interested in the boundary of the achievable region, characterized by the maximal  $s_x$  for a given  $s_z$ .

If  $s_z > r_z$ , Eq. (33) guarantees that Eq. (32) is satisfied. A *y-z*-preserving operation fulfilling Eq. (33) with equality is given by the Kraus operators

$$K_1 = \begin{pmatrix} a_1 & 0 \\ 0 & b_1 \end{pmatrix}, \quad K_2 = \begin{pmatrix} 0 & b_2 \\ a_2 & 0 \end{pmatrix}, \quad (34)$$

where the parameters  $a_i$  and  $b_i$  are chosen as

$$a_1 = \cos \frac{\theta - \nu}{2}, \quad a_2 = \sin \frac{\theta - \nu}{2}, \quad (35a)$$

$$b_1 = \sin \frac{\theta + \nu}{2}, \quad b_2 = \cos \frac{\theta + \nu}{2}, \quad (35b)$$

with  $\nu = \arctan[r_z \tan \theta]$  and parameter  $\theta$  is in the range  $[0, \frac{\pi}{2}]$ . By varying  $\theta$  it is possible to attain any value for  $s_z$  in the

range  $[r_z, 1]$ . This proves that for  $s_z > r_z$  the boundary of the achievable region is characterized by Eq. (33).

For  $s_z \leq r_z$  Eq. (32) ensures that Eq. (33) is fulfilled. The boundary of the achievable region is then obtained by the  $y$ - $z$ -preserving operation

$$\Lambda[\rho] = (1 - p)\rho + p\sigma_x\rho\sigma_x \quad (36)$$

with  $p$  in the range  $[0, 1/2]$ . This proves that for  $s_z \leq r_z$  the boundary of the achievable region is determined by Eq. (32).  $\square$

Equipped with these results, we are now ready to prove Eqs. (4) of the main text. Since rotations around the  $y$ -axis correspond to real unitaries, we can without loss of generality assume that the initial and the final state have Bloch vectors in the  $y$ - $z$  plane. It is thus enough to prove the statement for

$$s_y^2 \leq r_y^2 \quad (37a)$$

$$\frac{1 - s_z^2}{s_y^2} \geq \frac{1 - r_z^2}{r_y^2}. \quad (37b)$$

The proof of the theorem now directly follows from Lemma 2 by symmetry, exchanging the  $x$  and  $y$  directions.

## B. Proof of Theorem 1

The proof will use properties of pure states within imaginarity theory (see Section D) and geometric imaginarity  $\mathcal{I}_g$  (see Section E). Since  $\mathcal{I}_g$  is a strong imaginarity monotone, the transition probability  $P(\rho \rightarrow \sigma)$  is bounded as [see also Eq. (17) in the main text]:

$$P(\rho \rightarrow \sigma) \leq \frac{\mathcal{I}_g(\rho)}{\mathcal{I}_g(\sigma)}. \quad (38)$$

In the case of pure states we can use the results from Section E to obtain

$$P(|\psi\rangle \rightarrow |\phi\rangle) \leq \frac{1 - |\langle\psi^*|\psi\rangle|}{1 - |\langle\phi^*|\phi\rangle|}. \quad (39)$$

We will now consider the case

$$|\langle\psi^*|\psi\rangle| \geq |\langle\phi^*|\phi\rangle|, \quad (40)$$

and show that there exists a real operation saturating the bound (39). To see this, we first apply a real orthogonal transformation to the state  $|\psi\rangle$ , bringing it into the form

$$|\psi'\rangle = \sqrt{\frac{1 + |\langle\psi^*|\psi\rangle|}{2}}|0\rangle + i\sqrt{\frac{1 - |\langle\psi^*|\psi\rangle|}{2}}|1\rangle, \quad (41)$$

see Section D. Then, we apply a real operation with the Kraus operators

$$K_0 = \begin{pmatrix} a & 0 \\ 0 & 1 \end{pmatrix}, \quad K_1 = \sqrt{1 - K_0^2}, \quad (42)$$

where  $a$  is defined as

$$a = \sqrt{\frac{1 - |\langle\psi^*|\psi\rangle|}{1 - |\langle\phi^*|\phi\rangle|}} \times \frac{1 + |\langle\phi^*|\phi\rangle|}{1 + |\langle\psi^*|\psi\rangle|}. \quad (43)$$

Note that  $a \leq 1$  by Eq. (40). As it can be verified by inspection, the Kraus operator  $K_0$  transforms  $|\psi'\rangle$  into the state

$$|\phi'\rangle = \sqrt{\frac{1 + |\langle\phi^*|\phi\rangle|}{2}}|0\rangle + i\sqrt{\frac{1 - |\langle\phi^*|\phi\rangle|}{2}}|1\rangle, \quad (44)$$

with probability

$$p = \frac{1 - |\langle\psi^*|\psi\rangle|}{1 - |\langle\phi^*|\phi\rangle|}. \quad (45)$$

Note that  $|\phi'\rangle$  is equivalent to the desired state  $|\phi\rangle$  up to a real orthogonal transformation, see Section D.

For the remaining case  $|\langle\psi^*|\psi\rangle| < |\langle\phi^*|\phi\rangle|$ , the transformation  $|\psi\rangle \rightarrow |\phi\rangle$  can be achieved with unit probability [15].

## C. Proof of Theorem 2

We will now prove that for any quantum state  $\rho$  the fidelity of imaginarity can be written as

$$F_1(\rho) = \frac{1}{2}[1 + \mathcal{I}_R(\rho)]. \quad (46)$$

Here,  $\mathcal{I}_R$  is the robustness of imaginarity, defined as

$$\mathcal{I}_R(\rho) = \min_{\tau} \left\{ s > 0 : \frac{\rho + s\tau}{1 + s} \in \mathcal{R} \right\}, \quad (47)$$

where the minimum is taken over all quantum states  $\tau$ .

From the definition of  $\mathcal{I}_R$ , we can write  $\rho$  as

$$\rho = [1 + \mathcal{I}_R(\rho)]\delta - \mathcal{I}_R(\rho)\tau, \quad (48)$$

with some quantum state  $\tau$  and a real state  $\delta$ . By applying a real operation  $\Lambda$  on both sides we obtain

$$\langle \hat{\tau} | \Lambda(\rho) | \hat{\tau} \rangle = [1 + \mathcal{I}_R(\rho)]\langle \hat{\tau} | \Lambda(\delta) | \hat{\tau} \rangle - \mathcal{I}_R(\rho)\langle \hat{\tau} | \Lambda(\tau) | \hat{\tau} \rangle. \quad (49)$$

Since  $\Lambda$  is a real operation, we have  $\Lambda(\delta) \in \mathcal{R}$ . Noting that for any real state  $\delta \in \mathcal{R}$  it holds that  $\langle \hat{\tau} | \delta | \hat{\tau} \rangle \leq \frac{1}{2}$ , we have

$$\langle \hat{\tau} | \Lambda(\delta) | \hat{\tau} \rangle \leq \frac{1}{2}, \quad (50)$$

which proves the bound

$$\langle \hat{\tau} | \Lambda(\rho) | \hat{\tau} \rangle \leq \frac{1}{2}[1 + \mathcal{I}_R(\rho)]. \quad (51)$$

We will now show that this bound is achievable by a real operation  $\Lambda$ . Given a general quantum state, it is always possible to decompose it as [15]

$$\rho = \text{Re}(\rho) + i\text{Im}(\rho), \quad (52)$$

where  $\text{Re}(\rho) = \frac{1}{2}(\rho + \rho^T)$  is a real quantum state and  $\text{Im}(\rho) = \frac{1}{2i}(\rho - \rho^T)$  is a real anti-symmetric matrix. By spectral theorem  $\text{Im}(\rho)$  has an even rank  $2r$  and there is a real orthogonal matrix  $O$  such that  $O\text{Im}(\rho)O^T$  is block-diagonal [51, p. 136]:

$$O\text{Im}\rho O^T = \mathbf{0}_{d-2r} \bigoplus_{k=1}^r \lambda_k \begin{pmatrix} 0 & 1 \\ -1 & 0 \end{pmatrix}, \quad (53)$$

where  $\lambda_k > 0$ .

If the dimension is even, we now define a real operation  $\Lambda$  via the real Kraus operators

$$K_m = |1\rangle\langle 2m| + |0\rangle\langle 2m+1|, \quad m = 0, 1, \dots, d/2-1. \quad (54)$$

For odd dimension, the Kraus operators  $K_m$  are defined in the same way for  $m \leq \lfloor d/2 \rfloor - 1$ , and we further define

$$K_{\lfloor d/2 \rfloor} = |0\rangle\langle d-1|. \quad (55)$$

Let now  $O$  be a real orthogonal matrix such that  $O\text{Im}(\rho)O^T$  is block-diagonal as in Eq. (53). We see that  $\Lambda[O\text{Re}(\rho)O^T]$  is a real single-qubit state, which implies that

$$\langle \hat{\dagger} | \Lambda[O\text{Re}(\rho)O^T] | \hat{\dagger} \rangle = \frac{1}{2}. \quad (56)$$

Moreover, we have

$$\Lambda[O\text{Im}(\rho)O^T] = \left( \sum_{m=0}^{\lfloor d/2 \rfloor - 1} \lambda_m \right) (|1\rangle\langle 0| - |0\rangle\langle 1|). \quad (57)$$

The fidelity of the final state with the maximally imaginary state can now be evaluated as follows:

$$\begin{aligned} \langle \hat{\dagger} | \Lambda[O\rho O^T] | \hat{\dagger} \rangle &= \langle \hat{\dagger} | \Lambda[O\text{Re}(\rho)O^T] | \hat{\dagger} \rangle \\ &\quad + i \langle \hat{\dagger} | \Lambda[O\text{Im}(\rho)O^T] | \hat{\dagger} \rangle \\ &= \frac{1}{2} (1 + 2 \sum_m \lambda_m). \end{aligned} \quad (58)$$

To complete the proof, note that the robustness of imaginarity can be expressed as (see Section F)

$$\mathcal{I}_R(\rho) = \frac{1}{2} \|\rho - \rho^T\|_1 = \|\text{Im}(\rho)\|_1 = 2 \sum_m \lambda_m. \quad (59)$$

Using this result in Eq. (58), we obtain

$$\langle \hat{\dagger} | \Lambda[O\rho O^T] | \hat{\dagger} \rangle = \frac{1}{2} [1 + \mathcal{I}_R(\rho)]. \quad (60)$$

In summary, we proved that the fidelity  $\langle \hat{\dagger} | \Lambda(\rho) | \hat{\dagger} \rangle$  is upper-bounded by Eq. (51), and that this upper bound is achievable for any state  $\rho$  with a suitably chosen real operation  $\Lambda$ . This completes the proof of the theorem.

#### D. Pure states in imaginarity theory

We will now show that in the resource theory of imaginarity any pure state can be expressed in a simple form. Recalling

that the definition of imaginarity is basis dependent, we define complex conjugation of a state  $|\psi\rangle$  as follows:

$$|\psi^*\rangle = \sum_j c_j^* |j\rangle, \quad (61)$$

where  $\{|j\rangle\}$  is the reference basis, and  $c_j = \langle j|\psi\rangle$ . The states  $|\psi\rangle$  and  $|\psi^*\rangle$  can also be expressed as

$$|\psi\rangle = a|\gamma_1\rangle + ib|\gamma_2\rangle, \quad (62a)$$

$$|\psi^*\rangle = a|\gamma_1\rangle - ib|\gamma_2\rangle, \quad (62b)$$

where  $a$  and  $b$  are real numbers with  $a^2 + b^2 = 1$ , and  $|\gamma_i\rangle$  are real states. Equipped with these tools, we are now ready to prove the following proposition.

**Proposition 1.** *For any pure state  $|\psi\rangle$  there exists a real orthogonal matrix  $O$  such that*

$$O|\psi\rangle = \sqrt{\frac{1 + |\langle\psi^*|\psi\rangle|}{2}} |0\rangle + i \sqrt{\frac{1 - |\langle\psi^*|\psi\rangle|}{2}} |1\rangle. \quad (63)$$

*Proof.* In the first step, note that for any two real states  $|\gamma_1\rangle$  and  $|\gamma_2\rangle$  there exists a real orthogonal matrix  $O$  such that

$$O|\gamma_1\rangle = |0\rangle, \quad (64)$$

$$O|\gamma_2\rangle = \cos \theta |0\rangle + \sin \theta |1\rangle, \quad (65)$$

where  $\cos \theta = \langle \gamma_1 | \gamma_2 \rangle$ . Applying  $O$  to the state  $|\psi\rangle$  gives us

$$O|\psi\rangle = (a + ib \cos \theta) |0\rangle + ib \sin \theta |1\rangle. \quad (66)$$

Since the state  $O|\psi\rangle$  is effectively a single-qubit state, we can associate a Bloch vector  $\mathbf{r}$  with it, with coordinates

$$\begin{aligned} r_x &= b^2 \sin(2\theta), \\ r_y &= 2ab \sin(\theta), \\ r_z &= a^2 + b^2 \cos(2\theta). \end{aligned} \quad (67)$$

Let now  $O'$  be a real orthogonal transformation, such that the Bloch vector  $\mathbf{s}$  of the state  $O' O |\psi\rangle$  is in the positive  $y$ - $z$  plane. Since  $|\mathbf{s}| = 1$ , we can give the coordinates of  $\mathbf{s}$  as follows:

$$\begin{aligned} s_x &= 0, & s_y &= |r_y|, \\ s_z &= \sqrt{1 - r_y^2} = \sqrt{1 - 4a^2b^2 + 4a^2b^2 \cos^2 \theta}. \end{aligned} \quad (68)$$

From Eqs. (62) we further obtain

$$a|\gamma_1\rangle = \frac{|\psi\rangle + |\psi^*\rangle}{2}, \quad (69a)$$

$$b|\gamma_2\rangle = \frac{|\psi\rangle - |\psi^*\rangle}{2i}. \quad (69b)$$

These results allow us to express  $a^2$  and  $b^2$  as

$$a^2 = \left| \frac{|\psi\rangle + |\psi^*\rangle}{2} \right|^2 = \frac{1}{4} (2 + \langle \psi^* | \psi \rangle + \langle \psi | \psi^* \rangle), \quad (70)$$

$$b^2 = \left| \frac{|\psi\rangle - |\psi^*\rangle}{2i} \right|^2 = \frac{1}{4} (2 - \langle \psi^* | \psi \rangle - \langle \psi | \psi^* \rangle). \quad (71)$$

Recalling that  $\cos \theta = \langle \gamma_1 | \gamma_2 \rangle$  we arrive at

$$ab \cos \theta = ab \langle \gamma_1 | \gamma_2 \rangle = \frac{1}{4i} (\langle \psi^* | \psi \rangle - \langle \psi | \psi^* \rangle). \quad (72)$$

Using these results, we can simplify Eqs. (68) as follows:

$$s_x = 0, \quad s_y = \sqrt{1 - |\langle \psi^* | \psi \rangle|^2}, \quad s_z = |\langle \psi^* | \psi \rangle|. \quad (73)$$

The pure state corresponding to the Bloch vector  $\mathbf{s}$  is given by Eq. (63).  $\square$

### E. Geometric imaginarity

For a pure state  $|\psi\rangle$  we define the geometric imaginarity as

$$\mathcal{I}_g(|\psi\rangle) = 1 - \max_{|\phi\rangle \in \mathcal{R}} |\langle \phi | \psi \rangle|^2. \quad (74)$$

In the following proposition we give a closed expression for the geometric imaginarity of pure states.

**Proposition 2.** *The geometric imaginarity of a pure state  $|\psi\rangle$  is given as*

$$\mathcal{I}_g(|\psi\rangle) = \frac{1 - |\langle \psi^* | \psi \rangle|}{2}. \quad (75)$$

*Proof.* By definition, geometric imaginarity is invariant under real orthogonal transformations. Using Proposition 1 it follows that

$$\mathcal{I}_g(|\psi\rangle) = \mathcal{I}_g\left(\sqrt{\frac{1 + |\langle \psi^* | \psi \rangle|}{2}}|0\rangle + i\sqrt{\frac{1 - |\langle \psi^* | \psi \rangle|}{2}}|1\rangle\right). \quad (76)$$

To complete the proof, we will now evaluate  $\mathcal{I}_g$  for any state of the form

$$|\mu\rangle = a_0|0\rangle + ia_1|1\rangle \quad (77)$$

with  $a_0 \geq a_1 \geq 0$  and  $a_0^2 + a_1^2 = 1$ . For any real state  $|\nu\rangle = \sum_j b_j|j\rangle$  we have

$$|\langle \nu | \mu \rangle|^2 = |a_0 b_0 + ia_1 b_1|^2 = a_0^2 b_0^2 + a_1^2 b_1^2 \leq a_0^2, \quad (78)$$

where the inequality follows from the fact that  $\sum_j b_j^2 = 1$ . Since  $|\langle 0 | \mu \rangle|^2 = a_0^2$ , we conclude that

$$\max_{|\nu\rangle \in \mathcal{R}} |\langle \nu | \mu \rangle|^2 = a_0^2, \quad (79)$$

and thus  $\mathcal{I}_g(|\mu\rangle) = a_0^2$ .  $\square$

For mixed states, we define  $\mathcal{I}_g$  as the minimal average imaginarity, minimized over all decompositions of the state:

$$\mathcal{I}_g(\rho) = \min \sum_j p_j \mathcal{I}_g(|\psi_j\rangle). \quad (80)$$

From the definition we see that  $\mathcal{I}_g$  is convex:

$$\mathcal{I}_g\left(\sum_j p_j \rho_j\right) \leq \sum_j p_j \mathcal{I}_g(\rho_j). \quad (81)$$

We will now prove that geometric imaginarity does not increase under real operations on average, i.e.,

$$\sum_j q_j \mathcal{I}_g(\sigma_j) \leq \mathcal{I}_g(\rho), \quad (82)$$

where the probabilities  $q_j$  and states  $\sigma_j$  are obtained from  $\rho$  by means of a real operation, i.e.,

$$q_j = \text{Tr}[K_j \rho K_j^\dagger], \quad (83a)$$

$$\sigma_j = \frac{K_j \rho K_j^\dagger}{q_j} \quad (83b)$$

with real Kraus operators  $K_j$ .

To prove Eq. (82) in general, we will first prove it for pure states. By Proposition 1, it is enough to prove it for states  $|\alpha\rangle = \cos \alpha |0\rangle + i \sin \alpha |1\rangle$  with  $\alpha \in [0, \pi/4]$ , for which the geometric imaginarity is given by  $\mathcal{I}_g(|\alpha\rangle) = \sin^2 \alpha$ . For a pure initial state, all post-measurement states  $\sigma_j$  are also pure. Thus, proving Eq. (82) for pure states reduces to proving the inequality

$$\sum_j \max_{|\phi_j\rangle \in \mathcal{R}} |\langle \phi_j | K_j | \alpha \rangle|^2 \geq \cos^2 \alpha, \quad (84)$$

where  $\{K_j\}$  is a set of real Kraus operators. To prove Eq. (84), we first note that

$$\sum_j \max_{|\phi_j\rangle \in \mathcal{R}} |\langle \phi_j | K_j | \alpha \rangle|^2 \geq \sum_j \frac{|\langle 0 | K_j^T K_j | \alpha \rangle|^2}{s_j}, \quad (85)$$

where we introduced

$$s_j = \langle 0 | K_j^T K_j | 0 \rangle. \quad (86)$$

Recalling that all Kraus operators  $K_j$  are real and using the explicit form of  $|\alpha\rangle$  we obtain

$$\begin{aligned} |\langle 0 | K_j^T K_j | \alpha \rangle|^2 &= |\langle 0 | K_j^T K_j | 0 \rangle|^2 \cos^2 \alpha \\ &\quad + |\langle 0 | K_j^T K_j | 1 \rangle|^2 \sin^2 \alpha \\ &\geq |\langle 0 | K_j^T K_j | 0 \rangle|^2 \cos^2 \alpha, \end{aligned} \quad (87)$$

which further implies that

$$\sum_j \max_{|\phi_j\rangle \in \mathcal{R}} |\langle \phi_j | K_j | \alpha \rangle|^2 \geq \sum_j \frac{|\langle 0 | K_j^T K_j | 0 \rangle|^2}{s_j} \cos^2 \alpha. \quad (88)$$

Using the definition of  $s_j$  in Eq. (86) and the fact that  $\sum_j K_j^T K_j = \mathbb{1}$ , we obtain the desired inequality (84).

The above arguments prove that  $\mathcal{I}_g$  satisfies Eq. (82) when  $\rho$  is pure. To extend this result to mixed states, consider an optimal decomposition of a mixed state  $\rho = \sum_j p_j |\psi_j\rangle \langle \psi_j|$ , such that

$$\mathcal{I}_g(\rho) = \sum_j p_j \mathcal{I}_g(|\psi_j\rangle). \quad (89)$$

Introducing the quantity  $s_{jk} = \langle \psi_k | K_j^T K_j | \psi_k \rangle$  we obtain

$$\begin{aligned} \sum_j q_j \mathcal{I}_g \left( \frac{K_j \rho K_j^T}{q_j} \right) &= \sum_j q_j \mathcal{I}_g \left( \sum_k p_k \frac{K_j | \psi_k \rangle \langle \psi_k | K_j^T}{q_j} \right) \\ &= \sum_j q_j \mathcal{I}_g \left( \sum_k \frac{p_k s_{jk}}{q_j} \times \frac{K_j | \psi_k \rangle \langle \psi_k | K_j^T}{s_{jk}} \right) \\ &\leq \sum_{j,k} p_k s_{jk} \mathcal{I}_g \left( \frac{K_j | \psi_k \rangle \langle \psi_k | K_j^T}{s_{jk}} \right) \\ &\leq \sum_j p_j \mathcal{I}_g (| \psi_j \rangle) = \mathcal{I}_g(\rho), \end{aligned} \quad (90)$$

where in the first inequality we used the facts that  $\mathcal{I}_g$  is convex. This completes the proof of Eq. (82) for all mixed states.

## F. Robustness of imaginarity

We recall that the robustness of imaginarity is defined as

$$\mathcal{I}_R(\rho) = \min_{\tau} \left\{ s > 0 : \frac{\rho + s\tau}{1+s} \in \mathcal{R} \right\}, \quad (91)$$

where the minimum is taken over all quantum states  $\tau$ . The following proposition gives a closed expression for the robustness of imaginarity of any quantum state  $\rho$ .

**Proposition 3.** *The robustness of imaginarity is equal to*

$$\mathcal{I}_R(\rho) = \frac{1}{2} \|\rho - \rho^T\|_1. \quad (92)$$

*Proof.* Let  $\tau^*$  be a quantum state achieving the minimum in Eq. (91). Then, the matrix  $\rho + \mathcal{I}_R(\rho)\tau^*$  is real and Hermitian, and thus

$$\rho + \mathcal{I}_R(\rho)\tau^* = \rho^T + \mathcal{I}_R(\rho)(\tau^*)^T. \quad (93)$$

We can now obtain a lower bound on the robustness of imaginarity as follows:

$$\|\rho - \rho^T\|_1 = \mathcal{I}_R(\rho) \|(\tau^*)^T - \tau^*\|_1 \leq 2\mathcal{I}_R(\rho), \quad (94)$$

where we used the fact that  $\|(\tau^*)^T - \tau^*\|_1 \leq \|(\tau^*)^T\|_1 + \|\tau^*\|_1 = 2$ . Thus, we have the bound

$$\mathcal{I}_R(\rho) \geq \frac{1}{2} \|\rho - \rho^T\|_1. \quad (95)$$

To complete the proof, we will present a state  $\tau^*$  such that  $\rho + s\tau^*$  is a real matrix with  $s = \frac{1}{2} \|\rho - \rho^T\|_1$ . To see this, recall that there exists a real orthogonal matrix  $O$  such that  $O \text{Im} \rho O^T$  is block-diagonal as in Eq. (53) with coefficients  $\lambda_m \geq 0$ . If the dimension of the Hilbert space is even, we define  $\tau^*$  to be a block-diagonal matrix of the form

$$\tau^* = \frac{1}{2 \sum_m \lambda_m} O^T \begin{pmatrix} \lambda_1 & -i\lambda_1 \\ i\lambda_1 & \lambda_1 \\ & \lambda_2 & -i\lambda_2 \\ & i\lambda_2 & \lambda_2 \\ & & \ddots \\ & & & \lambda_k & -i\lambda_k \\ & & & i\lambda_k & \lambda_k \\ 0 & 0 & 0 & \dots & 0 & 0 & 0 \end{pmatrix} O. \quad (96)$$

Note that  $\rho + 2 \sum_m \lambda_m \tau^*$  is a real matrix, and moreover

$$\frac{1}{2} \|\rho - \rho^T\|_1 = \|\text{Im} \rho\|_1 = 2 \sum_m \lambda_m. \quad (97)$$

This completes the proof for Hilbert space with even dimension. For odd dimension, the proof follows the same lines of reasoning, if we define the state  $\tau^*$  as

$$\tau^* = \frac{1}{2 \sum_m \lambda_m} O^T \begin{pmatrix} \lambda_1 & -i\lambda_1 & & & & & 0 \\ i\lambda_1 & \lambda_1 & & & & & 0 \\ & & \lambda_2 & -i\lambda_2 & & & 0 \\ & & i\lambda_2 & \lambda_2 & & & 0 \\ & & & & \ddots & & \vdots \\ & & & & & \lambda_k & -i\lambda_k \\ & & & & & i\lambda_k & \lambda_k \\ 0 & 0 & 0 & 0 & \dots & 0 & 0 & 0 \end{pmatrix} O. \quad (98)$$

This completes the proof of the proposition.  $\square$

For single-qubit states with Bloch vector  $\mathbf{r} = (r_x, r_y, r_z)$  the robustness of imaginarity simplifies to  $\mathcal{I}_R(\rho) = |\mathbf{r}_y|$ .

## G. Proof of Eq. (17)

Let  $\{K_n\}$  be a (possibly incomplete) set of Kraus operators which transform  $\rho$  to  $\sigma$ :

$$\sigma = \frac{\sum_n K_n \rho K_n^\dagger}{\text{Tr} [\sum_n K_n \rho K_n^\dagger]}. \quad (99)$$

We further introduce Kraus operators  $\{L_m\}$  which complete the set  $\{K_n\}$ , i.e.,

$$\sum_n K_n^\dagger K_n + \sum_m L_m^\dagger L_m = \mathbb{1}. \quad (100)$$

We define the probabilities

$$p_n = \text{Tr}[K_n \rho K_n^\dagger], \quad (101)$$

$$q_m = \text{Tr}[L_m \rho L_m^\dagger], \quad (102)$$

and post-measurement states

$$\sigma_n = \frac{K_n \rho K_n^\dagger}{p_n}, \quad (103)$$

$$\tau_m = \frac{L_m \rho L_m^\dagger}{q_m}. \quad (104)$$

In general it holds that  $P(\rho \rightarrow \sigma) \geq \sum_n p_n$ , and there exists a set of free Kraus operators  $\{K_n\}$  saturating this inequality. In the following, we assume that this is the case, i.e.,  $P(\rho \rightarrow \sigma) = \sum_n p_n$ . Using convexity and strong monotonicity of  $R$  it follows that

$$\begin{aligned} R(\rho) &\geq \sum_n p_n R(\sigma_n) + \sum_m q_m R(\tau_m) \geq \sum_n p_n R(\sigma_n) \\ &= P(\rho \rightarrow \sigma) \sum_n \frac{p_n}{P(\rho \rightarrow \sigma)} R(\sigma_n) \\ &\geq P(\rho \rightarrow \sigma) R(\sigma). \end{aligned} \quad (105)$$

This completes the proof.

## H. Decomposing real orthogonal unitaries into two-level transformations

It is well known that any  $m \times m$  unitary matrix can be written as a product of at most  $m(m-1)/2$  unitary matrices acting on two levels only. We will now show that a similar result also holds for real orthogonal matrices.

**Proposition 4.** *Any  $m \times m$  real orthogonal matrix can be written as a product of at most  $m(m-1)/2$  two-level real orthogonal matrices.*

*Proof.* The proof follows the same arguments as for unitary matrices, see e.g. [52, p. 189]. There, an explicit construction is presented for decomposing an  $m \times m$  unitary matrix  $U$  into  $m(m-1)/2$  two-level unitaries. If  $U$  is additionally real, all two-level unitaries constructed in the proof are also real.  $\square$

## I. Discrimination of bipartite real states

Any two orthogonal pure states  $|\psi\rangle^{AB}$  and  $|\phi\rangle^{AB}$  can be perfectly distinguished via LOCC [25]. We will now show that if the two states are additionally real, the task can be achieved with local real operations and classical communication.

**Proposition 5.** *Two real orthogonal pure quantum states  $|\psi\rangle^{AB}$  and  $|\phi\rangle^{AB}$  can be perfectly distinguished via local real operations and classical communication.*

*Proof.* The proof follows similar lines of reasoning as in Ref. [25]. Any two real pure states can be expanded as

$$|\psi\rangle^{AB} = \sum_{j=0}^{d-1} |j\rangle|a_j\rangle, \quad (106a)$$

$$|\phi\rangle^{AB} = \sum_{j=0}^{d-1} |j\rangle|b_j\rangle, \quad (106b)$$

where  $|a_j\rangle$  and  $|b_j\rangle$  are (unnormalized) real states and  $d = d_A$  is Alice's dimension. Without loss of generality we assume that  $d_A \leq d_B$ , where  $d_B$  is Bob's dimension.

We now consider the matrix  $C$  with elements

$$C_{jk} = \langle a_j|b_k\rangle. \quad (107)$$

Since  $|\psi\rangle^{AB}$  and  $|\phi\rangle^{AB}$  are orthogonal, we have

$$\text{Tr } C = 0. \quad (108)$$

If we apply a real orthogonal matrix  $O$  on Alice's side, the two states are transformed as

$$(O \otimes \mathbb{I})|\psi\rangle^{AB} = \sum_{k=0}^{d-1} |k\rangle \sum_{j=0}^{d-1} O_{kj}|a_j\rangle, \quad (109a)$$

$$(O \otimes \mathbb{I})|\phi\rangle^{AB} = \sum_{k=0}^{d-1} |k\rangle \sum_{j=0}^{d-1} O_{kj}|b_j\rangle. \quad (109b)$$

If now Alice applies a local von Neumann measurement in the computational basis, Bob is left with a (possibly unnormalized) state of the form

$$|\tilde{a}_k\rangle = \sum_j O_{kj}|a_j\rangle \quad \text{or} \quad |\tilde{b}_k\rangle = \sum_j O_{kj}|b_j\rangle. \quad (110)$$

This allows us to define a matrix  $\tilde{C}$  as follows:

$$\tilde{C}_{mn} = \langle \tilde{a}_m|\tilde{b}_n\rangle = \sum_{kl} O_{mk}\langle a_k|b_l\rangle O_{nl} = \sum_{kl} O_{mk}C_{kl}(O^T)_{ln}, \quad (111)$$

so we have  $\tilde{C} = OCO^T$ .

In the next step we will show that there exists a real orthogonal matrix  $O$  such that all diagonal elements of  $\tilde{C}$  become zero. This will complete the proof: if Alice applies  $O$  locally and performs a von Neumann measurement in the computational basis, Bob will find his system either in the state  $|\tilde{a}_j\rangle$  or  $|\tilde{b}_j\rangle$ . Bob can distinguish these states perfectly, since

$$\tilde{C}_{jj} = \langle \tilde{a}_j|\tilde{b}_j\rangle = 0. \quad (112)$$

Note that for any  $2 \times 2$  real matrix  $C$ , there always exists a real orthogonal  $2 \times 2$  matrix  $O$  such that the diagonal elements of  $OCO^T$  are equal to each other. Assume now that the dimension of Alice is a power of 2, i.e.,  $d_A = 2^k$ . This implies that  $C$  is a  $2^k \times 2^k$  real matrix. Our goal is to make all the diagonal elements of  $C$  zero by applying two-level real orthogonal rotations. Recalling that the trace of  $C$  is zero, our goal can be achieved by making all the diagonal elements equal.

To this end, we first group all diagonal elements of  $C$  into  $2^{k-1}$  pairs and apply  $2^{k-1}$  real orthogonal transformations, each acting on two levels. In this way we can obtain a new matrix  $C'$  with the property  $\text{Tr } C' = \text{Tr } C$  and the diagonal elements of  $C'$  are pairwise equal. Consider now two pairs of diagonal elements, e.g.

$$C'_{00} = C'_{11}, \quad C'_{22} = C'_{33}. \quad (113)$$

We can now apply two real orthogonal transformations, one acting on levels 0 and 2, and the other acting on levels 1 and 3. In this way, with a suitable choice of real orthogonal transformations, we can obtain a new matrix  $C''$  with the properties  $\text{Tr } C'' = \text{Tr } C$  and

$$C''_{00} = C''_{11} = C''_{22} = C''_{33}. \quad (114)$$

Proceeding in this way, we can make all diagonal elements equal to zero. This completes the proof for the case that the dimension of Alice's system is a power of 2.

If the dimension of Alice's system is not a power of 2, we can extend the dimension of Alice to be of the form  $2^k$ , thus extending the correlation matrix  $C$  with additional rows and columns having zero in all entries. All parts of the proof remain the same, which proves the statement for any dimension of Alice.  $\square$

## J. Experimental details

The experimental setup contains two modules: a state preparation and a measurement module. In the state preparation module, we can prepare several classes of two-photon

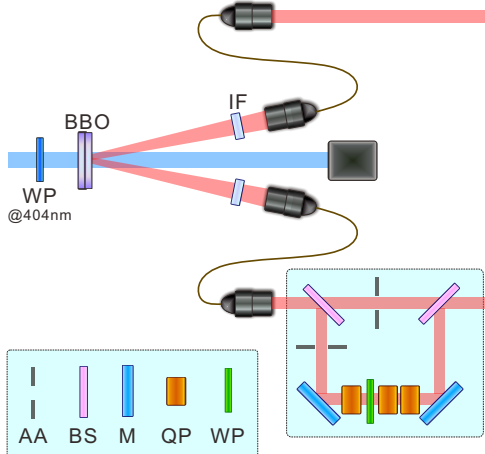


FIG. 5. **Experimental setup for preparing two-photon Werner states.** A two-photon entangled pure states  $|HH\rangle + |VV\rangle$  is generated via a SPDC process, following a unbalanced interferometer (light blue region). The optical elements are: WP, wave plate; BBO,  $\beta$ -BaB<sub>2</sub>O<sub>4</sub>; IF, interference filter; AA, adjustable aperture; BS, beam splitter; M, mirror; QP, quartz plate.

states. In particular, we can prepare all Bell states  $|\phi^\pm\rangle$ ,  $|\psi^\pm\rangle$ , Werner states  $p|\phi^+\rangle\langle\phi^+| + (1-p)\frac{1}{4}$ , mixed two-qubit states  $u|\phi^+\rangle\langle\phi^+| + (1-u)|\psi\rangle\langle\psi|$ , and maximally correlated states  $w|\phi^+\rangle\langle\phi^+| + (1-w)|\phi^-\rangle\langle\phi^-|$ . Fig. 5 illustrates the methods for experimentally generating Werner states, which can also be used to generate the four Bell states [45, 53]. Specifically, to generate  $|\phi^\pm\rangle$ , we need to drop the unbalanced interferometer (UI) part (the light blue region in Fig. 5), and set the angle of the wave plate (WP@404 nm) to  $50 \pm 22.5^\circ$ . To prepare  $|\psi^\pm\rangle$ , we need an additional wave plate in one of the arms to flip one of the photonic states.

To generate Werner states

$$\rho_p = p|\phi^+\rangle\langle\phi^+| + (1-p)\frac{1}{4}, \quad (115)$$

we make use of a technology named unbalanced Mach-Zehnder interferometer (the light blue region in Fig. 5), which is implemented on one of the entangled photon pairs. We use a variation of the technology presented in [45, 53, 54], with the parameter  $p$  controlled by adjusting two apertures in the UI.

To prepare the two-photon states  $\frac{1}{2}(u|\phi^+\rangle\langle\phi^+| + (1-u)|\psi\rangle\langle\psi| + |\phi^-\rangle\langle\phi^-|)$ , we use the ensemble average of a two-photon mixed state  $u|\phi^+\rangle\langle\phi^+| + (1-u)|\psi\rangle\langle\psi|$  and a pure state  $|\phi^-\rangle$ . The preparation of  $u|\phi^+\rangle\langle\phi^+| + (1-u)|\psi\rangle\langle\psi|$  and maximally correlated states is realized by placing adjustable quartz plates (QP) in either optical path (see Fig. 6). We first introduce the methods for preparing the former one. The two-qubit state can be written as

$$\rho_2 = p|\phi^+\rangle\langle\phi^+| + (1-p)\tilde{O}|\phi^+\rangle\langle\phi^+|\tilde{O}^T, \quad (116)$$

where  $\tilde{O} = \tilde{o} \otimes \mathbb{1}$  is some orthogonal matrix,  $\tilde{o} = R^{-1}(\theta)\sigma_z R(\theta)$ , and  $R(\theta)$  is a 2-dimensional rotation. Thus we can write

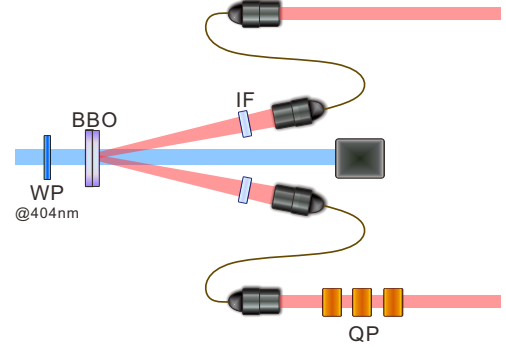


FIG. 6. **Experimental setup to prepare other classes of two-photon mixed states.** The preparations of  $u|\phi^+\rangle\langle\phi^+| + (1-u)|\psi\rangle\langle\psi|$  and maximally correlated states are shown.

Eq. (116) as

$$\rho_2 = R^{-1}(\theta) \left[ p|\tilde{\phi}^+\rangle\langle\tilde{\phi}^+| + (1-p)\sigma_z|\tilde{\phi}^+\rangle\langle\tilde{\phi}^+|\sigma_z \right] R(\theta), \quad (117)$$

where  $|\tilde{\phi}^+\rangle\langle\tilde{\phi}^+| = R(\theta)|\phi^+\rangle\langle\phi^+|R^{-1}(\theta)$ .

Note that  $p(\cdot) + (1-p)\sigma_z \cdot \sigma_z$  is the decoherence map. Then by Eq. (117), it is obvious that  $u|\phi^+\rangle\langle\phi^+| + (1-u)|\psi\rangle\langle\psi|$  can be realized by implementing a rotated local decoherence map on one subsystem. In particular, this is done by placing QPs in either path with rotation angles set to around  $20^\circ$ , after preparing a maximally entangled state  $|\phi^+\rangle$ . We can use similar methods to prepare the maximally correlated states by placing QPs with rotation angles set to  $0^\circ$ .

In the task of local state discrimination, we have to distinguish some mixed states by local projective measurements and classical communication. Because all the states to be distinguished are mixtures of several pure entangled states, we can either directly prepare them or use averages over ensembles of pure states.

The measurement module can perform all projective qubit measurements and produce corresponding coincident outcomes. In particular, we experimentally prepare the two bipartite states separately and compare the measurement outcomes. Here, we consider only projective measurements producing four outcomes experimentally; however, the results can be generalized to non-projective measurements. Let us consider two projective measurements along  $\alpha$  and  $\beta$  on Alice's and Bob's system, respectively, where  $\alpha$  and  $\beta$  are directions in the Bloch ball. Recall that any bipartite state of two qubits can be written as

$$\rho^{AB} = \frac{1}{4} \left( \mathbb{1} + \sum_j a_j \sigma_j^A \otimes \mathbb{1}^B + \mathbb{1}^A \otimes \sum_j b_j \sigma_j^B + \sum_{jk} E_{jk} \sigma_j^A \otimes \sigma_k^B \right). \quad (118)$$

There are four possible outcomes ++, +-,-+,-- for the two projective measurements. The probability for each outcome reads

$$P_{m_a, m_b} = \frac{1}{4} \left[ 1 + m_a \alpha \cdot \mathbf{a} + m_b \beta \cdot \mathbf{b} + m_a m_b \beta^T \cdot (E^T \alpha) \right], \quad (119)$$

where  $\mathbf{a} = (a_1, a_2, a_3)$ ,  $\mathbf{b} = (b_1, b_2, b_3)$ , as in Eq. (118), and  $m_a = \pm 1$ ,  $m_b = \pm 1$  denote measurement outcomes. The probability of distinguishing two states  $\{p, \rho^{AB}\}$  and  $\{\tilde{p}, \tilde{\rho}^{AB}\}$  under measurements along  $\mathbf{a}$  and  $\mathbf{b}$  is given by

$$p_{\text{succ}} = \sum_{j=-, k=-}^{+, +} \max \{p P_{jk}, \tilde{p} \tilde{P}_{jk}\}, \quad (120)$$

which can be evaluated as

$$p_{\text{succ}} = \frac{1}{2} \sum_{j=-, k=-}^{+, +} (p P_{jk} + \tilde{p} \tilde{P}_{jk} + |p P_{jk} - \tilde{p} \tilde{P}_{jk}|). \quad (121)$$

Substituting into Eq. (118) we obtain

$$\begin{aligned} p_{\text{succ}} &= \frac{1}{2} + \frac{1}{8} |\alpha \cdot \delta \mathbf{a} + \beta \cdot \delta \mathbf{b} + \beta^T \cdot (\Delta E^T \alpha)| \\ &+ \frac{1}{8} |\alpha \cdot \delta \mathbf{a} - \beta \cdot \delta \mathbf{b} - \beta^T \cdot (\Delta E^T \alpha)| \\ &+ \frac{1}{8} |\alpha \cdot \delta \mathbf{a} - \beta \cdot \delta \mathbf{b} + \beta^T \cdot (\Delta E^T \alpha)| \\ &+ \frac{1}{8} |\alpha \cdot \delta \mathbf{a} + \beta \cdot \delta \mathbf{b} - \beta^T \cdot (\Delta E^T \alpha)| \end{aligned} \quad (122)$$

where  $\delta \mathbf{a} = p \mathbf{a} - \tilde{p} \tilde{\mathbf{a}}$ ,  $\delta \mathbf{b} = p \mathbf{b} - \tilde{p} \tilde{\mathbf{b}}$  and  $\Delta E^T = p E^T - \tilde{p} \tilde{E}^T$ . Note that in our experiments, we have  $\delta \mathbf{a} = \delta \mathbf{b} = \mathbf{0}$  theoretically. Then  $p_{\text{succ}} = [1 + |\beta^T \cdot (\Delta E^T \alpha)|]/2$ . Thus ideally the maximum distinguishing probability is given by

$$p_{\text{succ}} = \frac{1}{2} + \frac{(\Delta E)_m}{2}, \quad (123)$$

where  $(\Delta E)_m$  is the maximum singular value of  $\Delta E^T$ .

For bipartite real states, we can write  $\Delta E^T$  as

$$\Delta E^T = \begin{pmatrix} e_{xx} & 0 & e_{xz} \\ 0 & e_{yy} & 0 \\ e_{zx} & 0 & e_{zz} \end{pmatrix}; \quad (124)$$

moreover, if both Alice and Bob can only use “real” measurement, then  $\alpha_y = \beta_y = 0$ . The maximum guessing probability is determined according to the maximum singular value of  $\begin{pmatrix} e_{xx} & e_{xz} \\ e_{zx} & e_{zz} \end{pmatrix}$ , which we denote as  $(\Delta e)_m$ . When  $e_{yy} > (\Delta e)_m$ , any non-zero amount of imaginarity in local measurement results in an advantage over all real measurements.

In our experiments, we measured the maximum success probabilities for four class of mixed states,

- (i)  $|\phi \rangle \langle \phi|^{AB} = |\phi^+ \rangle \langle \phi^+|$ ,
- $\rho_2^{AB} = \frac{1}{2} [u|\phi^+ \rangle \langle \phi^+| + (1-u)|\psi \rangle \langle \psi| + |\phi^- \rangle \langle \phi^-|]$ ,
- (ii)  $\rho_1^{AB} = p|\phi^+ \rangle \langle \phi^+| + (1-p)\frac{1}{4}$ ,
- $\rho_2^{AB} = \frac{1}{4} (|\phi^+ \rangle \langle \phi^+| + |\psi \rangle \langle \psi| + 2|\phi^- \rangle \langle \phi^-|)$ ,

$$\begin{aligned} \text{(iii)} \quad \rho_1^{AB} &= \frac{1}{2} (|\phi^- \rangle \langle \phi^-| + |\psi^+ \rangle \langle \psi^+|), \\ \rho_2^{AB} &= p|\phi^+ \rangle \langle \phi^+| + (1-p)\frac{1}{4}, \\ \text{(iv)} \quad \rho_1^{AB} &= \frac{1}{2} (|\phi^- \rangle \langle \phi^-| + |\psi^+ \rangle \langle \psi^+|), \\ \rho_2^{AB} &= \frac{1}{2} (1 + \sqrt{2a-1})|\phi^+ \rangle \langle \phi^+| + \frac{1}{2} (1 - \sqrt{2a-1})|\phi^- \rangle \langle \phi^-|, \end{aligned} \quad (125)$$

where  $|\psi\rangle = \psi_{00}|00\rangle + \psi_{01}|01\rangle + \psi_{10}|10\rangle + \psi_{11}|11\rangle$  is a non-trivial entangled pure state with  $\psi_{00} = -\psi_{11} \approx 0.54$  and  $\psi_{01} = \psi_{10} \approx 0.46$ , and the parameter  $a$  denotes the purity of the state  $\rho_2^{AB}$ .

For the states in (i), we can theoretically calculate the maximum guessing probability under local projective measurements and classical communications, which turns out to be

$$p_{\text{succ}} = 1 - \frac{u}{4}. \quad (126)$$

When restricted to real measurements, the maximum guessing probability is

$$\frac{1}{8} \left\{ 6 - p + \sqrt{2 + (-1)^{\frac{4}{9}} - (-1)^{\frac{5}{9}} + p \left[ -2 - (-1)^{\frac{4}{9}} + (-1)^{\frac{5}{9}} \right] + p^2} \right\} \quad (127)$$

which is less than  $1 - u/4$ . Here we used the principal value of the complex powers of  $-1$ . For the states in (ii), the theoretically calculated maximum guessing probability is given by

$$p_{\text{succ}} = \frac{5}{8} + \frac{p}{4}, \quad (128)$$

but, for

$$p < \frac{1}{8} \left[ -1 + \sqrt{5 + 4 \sin \frac{\pi}{18}} \right], \quad (129)$$

measurements with imaginary part will not provide any advantage.

Then for the states in (iii), maximum guessing probability is given by

$$p_{\text{succ}} = \frac{p}{4} + \frac{3}{4}, \quad (130)$$

while for real measurements, the upper bound is given by  $p/4 + 1/2$ .

Finally for the states in (iv), we can theoretically obtain the maximum guessing probability as

$$p_{\text{succ}} = \frac{3}{4} + \frac{\sqrt{2a-1}}{4}, \quad (131)$$

where  $a$  represents purity. For real measurements the probability can be evaluated as  $3/4$ .